Investigation of the influence of chirality and halogen atoms on the anticancer activity of enantiopure palladium(II) complexes derived from chiral amino-alcohol Schiff bases and 2-picolylamine

Hadi Amiri Rudbari[a,*], Nazanin Kordestani[a], Jose V. Cuevas-Vicario[b], Min Zhou[c], Thomas Efferth[c] Isabel Correia[d], Tanja Schirmeister[e], Fabian Barthels[e], Mohammed Enamullah[f], Alexandra R. Fernandes[g], Nicola Micale[h,*]

[a] *Department of Chemistry, University of Isfahan, Isfahan 81746-73441, Iran.*

[b] *Department of Chemistry, Universidad de Burgos, Pza. Misael Bañuelos s/n, E-09001 Burgos, Spain.*

[c] *Department of Pharmaceutical Biology, Institute of Pharmaceutical and Biomedical Sciences, Johannes Gutenberg University, Staudinger Weg 5, 55128 Mainz, Germany*

[d] *Centro de Química Estrutural, Departamento de Engenharia Química, Instituto Superior Técnico, Universidade de Lisboa, Av. Rovisco Pais 1, 1049-001 Lisboa, Portugal*

[e] *Department of Medicinal Chemistry, Institute of Pharmaceutical and Biomedical Sciences, Johannes Gutenberg University, Staudinger Weg 5, 55128 Mainz, Germany.*

[f] *Department of Chemistry, Jahangirnagar University, Dhaka1342, Bangladesh.*

[g] *UCIBIO, Departamento Ciências da Vida, Faculdade de Ciências e Tecnologia, Universidade NOVA de Lisboa, 2829-516 Caparica, Portugal.*

[h] *Department of Chemical, Biological, Pharmaceutical and Environmental Sciences, University of Messina, Viale Ferdinando Stagno D'Alcontres 31, I-98166 Messina, Italy.*

* Corresponding authors.

E-mail addresses: h.a.rudbari@sci.ui.ac.ir; hamiri1358@gmail.com (H. Amiri Rudbari), nmicale@unime.it (Nicola Micale)

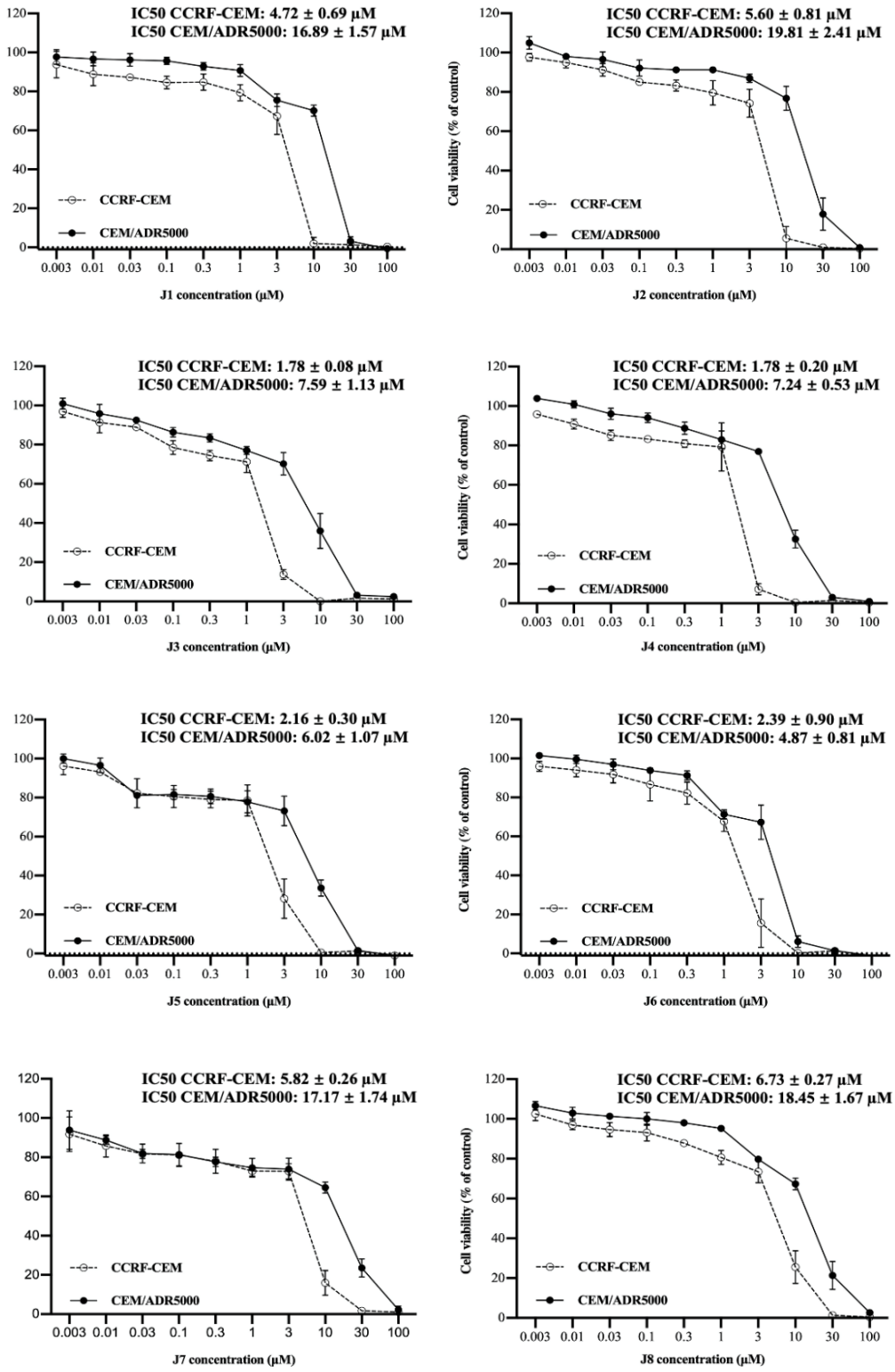

Fig. S1. Concentration-response curves of compounds **J1-J8** and doxorubicin (positive control) towards CCRF-CEM and CEM/ADR5000 cells. Resazurin assays were performed three times at 37 °C for 72 h.

Table S1: CCRF-CEM cell cycle distribution (%) after 24, 48 and 72 h treatment of the compound **J4** at concentrations of 0.5*IC_{50}, IC_{50}, 2*IC_{50}. In **J4** treatment, G2/M phase was also arrested in a concentration-dependent manner.

J4 24 h

	sub G1		G0/G1		S		G2/M	
	Mean	SD	Mean	SD	Mean	SD	Mean	SD
Control	0.7	0.5	50.4	4.8	30.9	0.3	17.9	5.4
0.5IC50	1.0	0.4	46.1	5.5	33.1	1.8	19.7	6.6
IC50	1.	0.7	47.8	5.3	30.6	3.2	19.9	6.6
2IC50	5.6	3.0	38.0	3.7	32.0	2.2	24.4	6.6

J4 48 h

	sub G1		G0/G1		S		G2/M	
	Mean	SD	Mean	SD	Mean	SD	Mean	SD
control	1.0	0.2	46.6	4.9	36.4	6.3	15.5	1.7
0.5IC50	2.33	1.8	50.3	6.5	30.2	7.3	17.2	2.4
IC50	1.4	0.0	49.6	2.6	27.8	0.3	21.2	2.3
2IC50	5.8	1.6	34.5	2.7	30.5	4.2	29.0	3.1

J4 72 h

	sub G1		G0/G1		S		G2/M	
	Mean	SD	Mean	SD	Mean	SD	Mean	SD
control	3.1	2.8	43.5	1.2	35.4	4.1	18.0	3.9
0.5IC50	5.9	6.3	41.6	2.3	36.9	3.2	15.6	4.4
IC50	4.7	3.1	45.3	1.8	38.2	4.6	11.7	2.5
2IC50	5.0	2.5	34.7	8.4	36.2	4.2	24.0	5.5

Table S2: CCRF-CEM cell cycle distribution (%) after 24 , 48 and 72 h treatment of the compound **J6** at concentrations of 0.5*IC_{50}, IC_{50}, 2*IC_{50}. In **J6** treatment, G2/M phase was also arrested in a concentration-dependent manner.

J6 24 h

	sub G1		G0/G1		S		G2/M	
	Mean	SD	Mean	SD	Mean	SD	Mean	SD
control	0.6	0.2	48.7	3.9	30.8	0.3	20.0	4.2
0.5IC50	1.3	0.4	43.9	2.9	30.5	2.4	24.2	5.5
IC50	2.6	0.8	45.2	5.0	29.2	3.2	23.1	6.5
2IC50	8.0	2.4	20.4	13.0	37.5	6.5	34.2	7.7

J6 48 h

	sub G1		G0/G1		S		G2/M	
	Mean	SD	Mean	SD	Mean	SD	Mean	SD
control	1.4	0.3	46.9	4.0	35.3	5.4	16.4	1.9
0.5IC50	1.3	0.6	41.6	7.9	36.5	6.1	20.6	5.8
IC50	1.3	0.7	29.1	12.9	35.9	8.7	23.4	4.3
2IC50	5.1	1.2	24.7	11.4	35.9	6.2	28.6	3.0

J6 72 h

	sub G1		G0/G1		S		G2/M	
	Mean	SD	Mean	SD	Mean	SD	Mean	SD
control	3.1	2.8	43.5	1.2	35.4	4.1	18.0	3.9
0.5IC50	3.5	1.7	40.9	3.9	37.9	3.3	17.6	3.2
IC50	2.4	1.2	38.2	4.8	39.7	2.7	19.9	2.7
2IC50	4.8	1.8	30.6	4.3	37.2	7.7	27.4	4.9

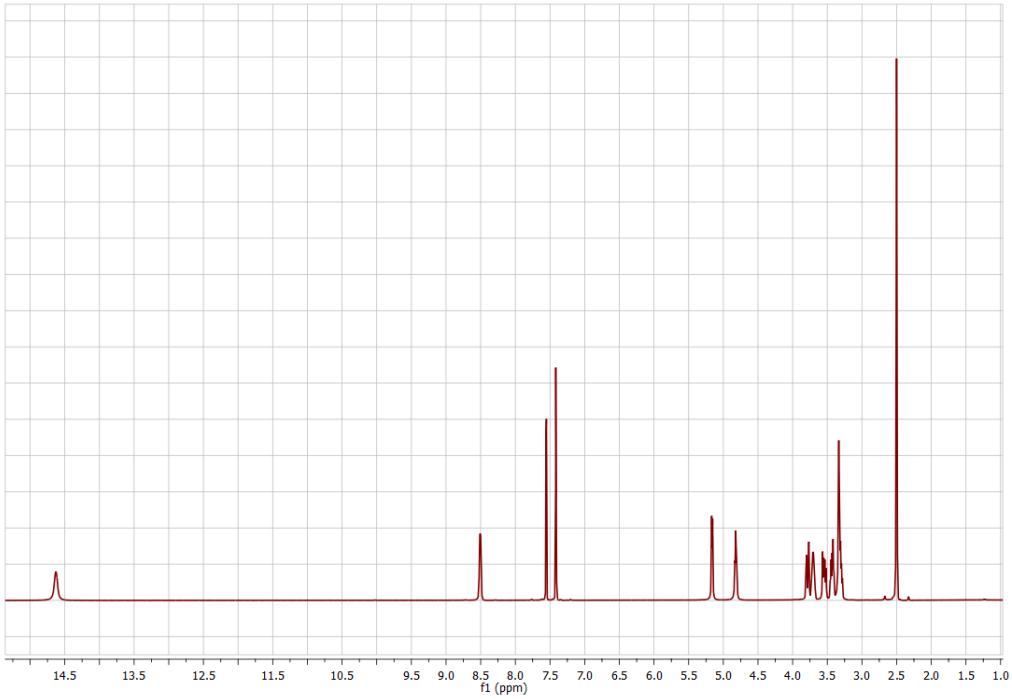

Fig. S2. ^{1}H NMR spectrum of **H*R*1** in DMSO-d_6.

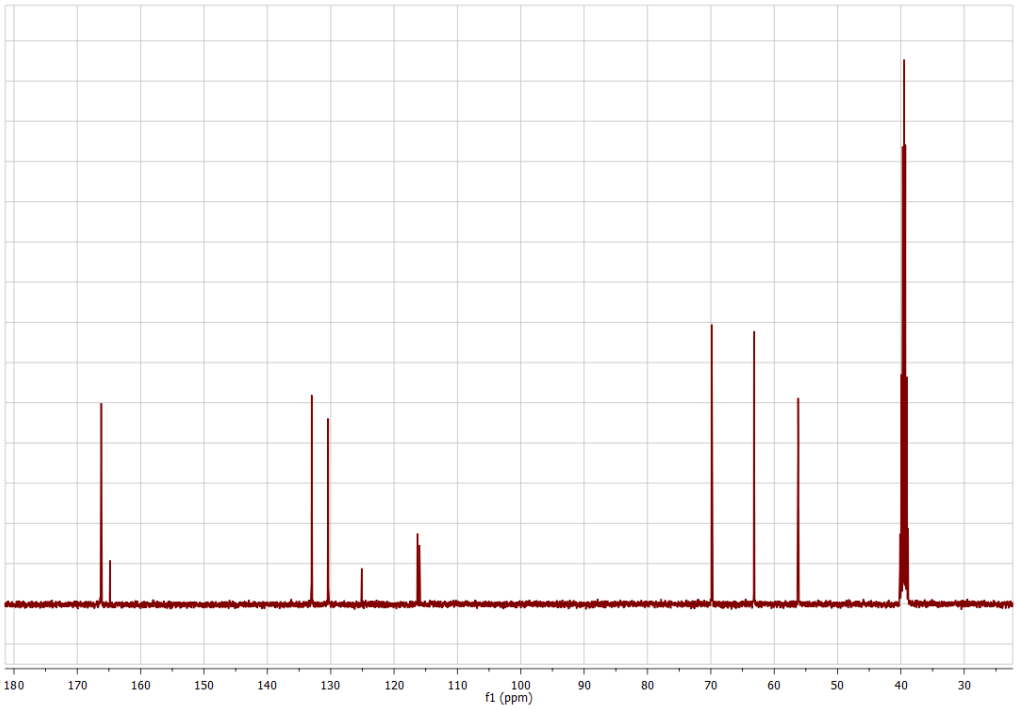

Fig. S3. ^{13}C NMR spectrum of **H*R*1** in DMSO-d_6.

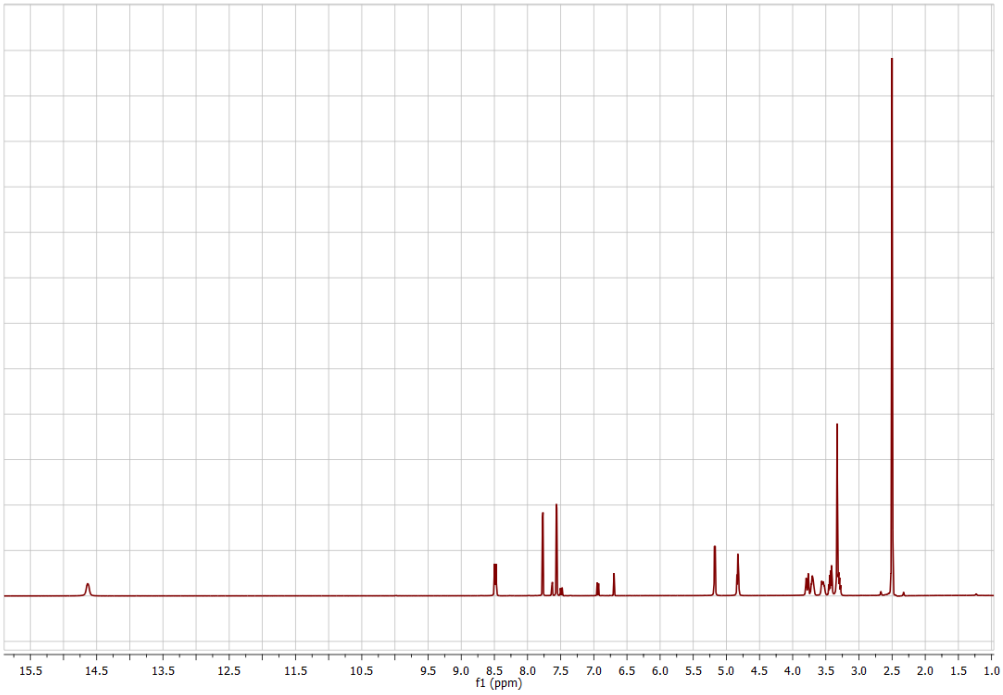

Fig. S4. ^{1}H NMR spectrum of **H*R*2** in DMSO-d_6.

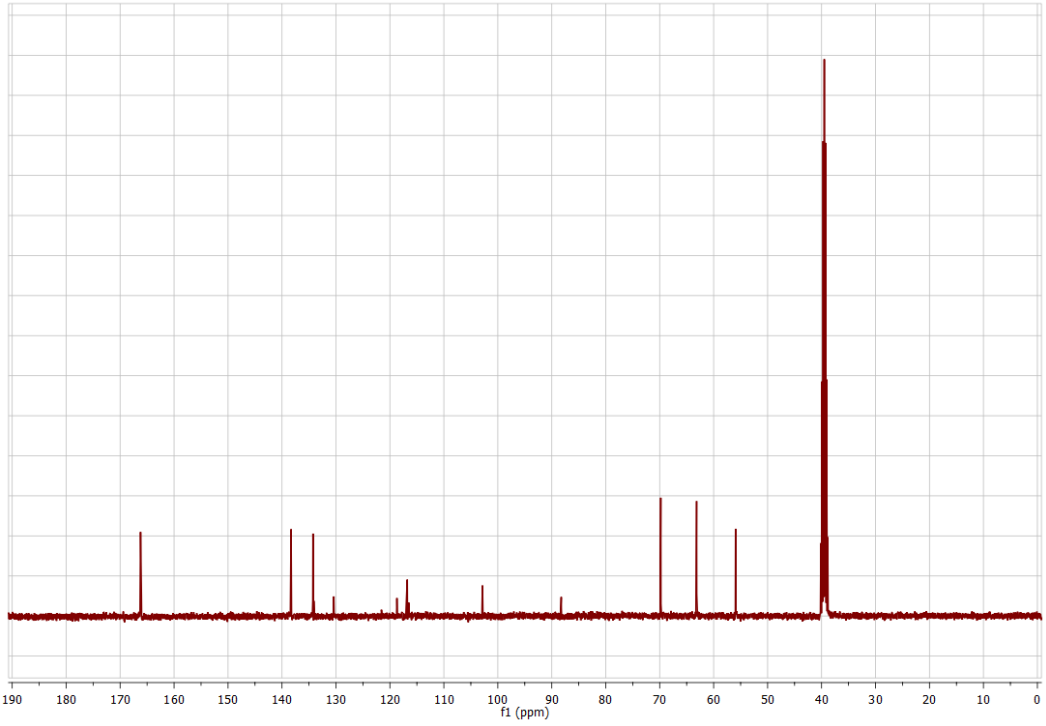

Fig. S5. ^{13}C NMR spectrum of **H*R*2** in DMSO-d_6.

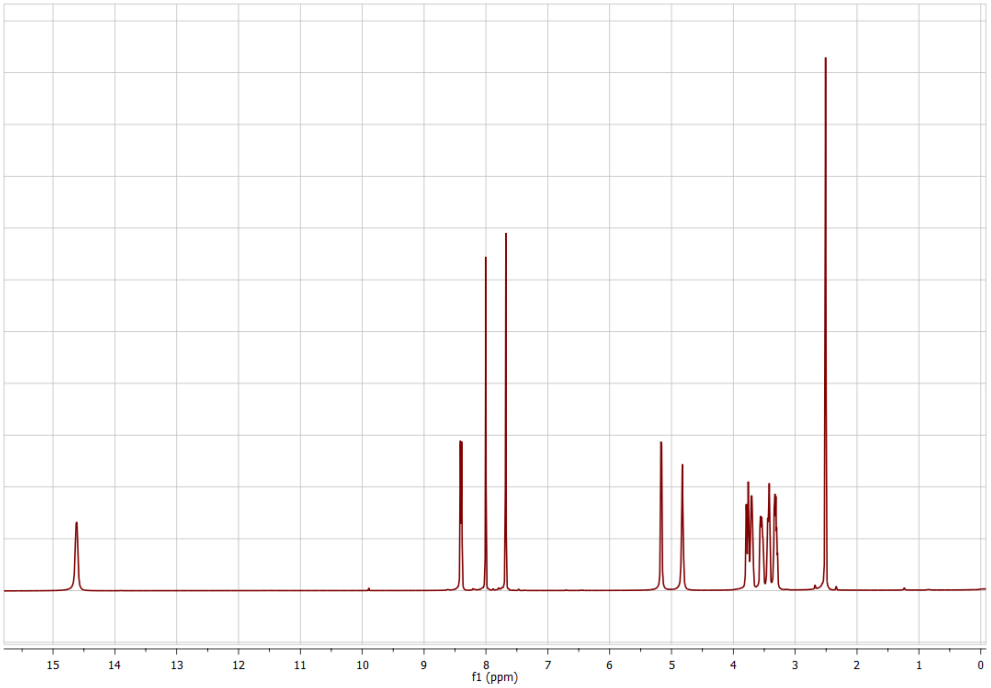

Fig. S6. ^{1}H NMR spectrum of **H*R*3** in DMSO-d_6.

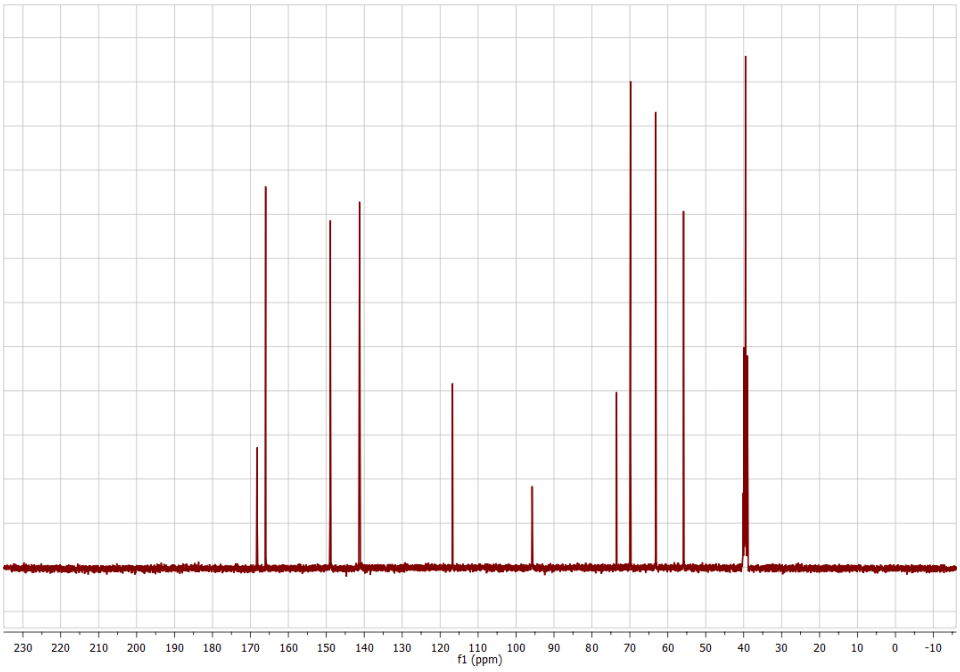

Fig. S7. ^{13}C NMR spectrum of **H*R*3** in DMSO-d_6.

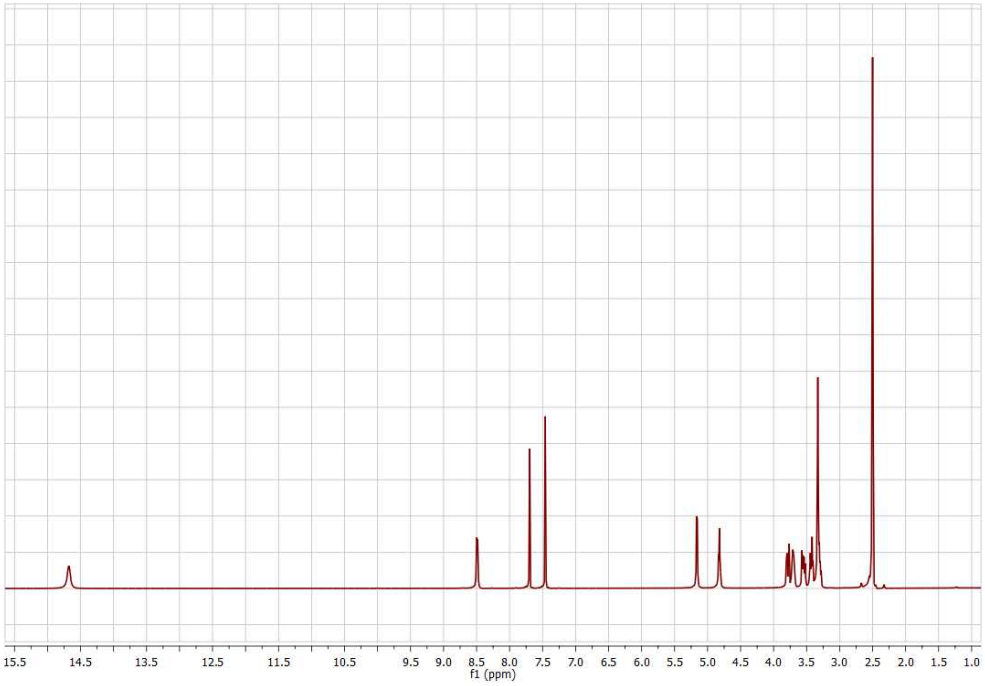

Fig. S8. ^{1}H NMR spectrum of **H*R*4** in DMSO-d_6.

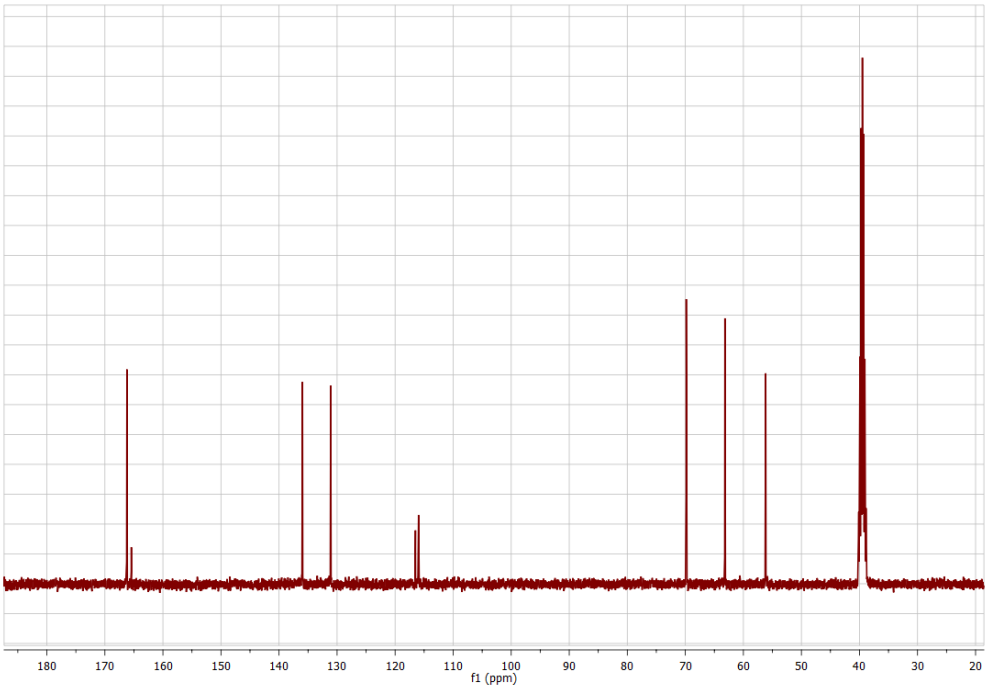

Fig. S9. ^{13}C NMR spectrum of **H*R*4** in DMSO-d_6.

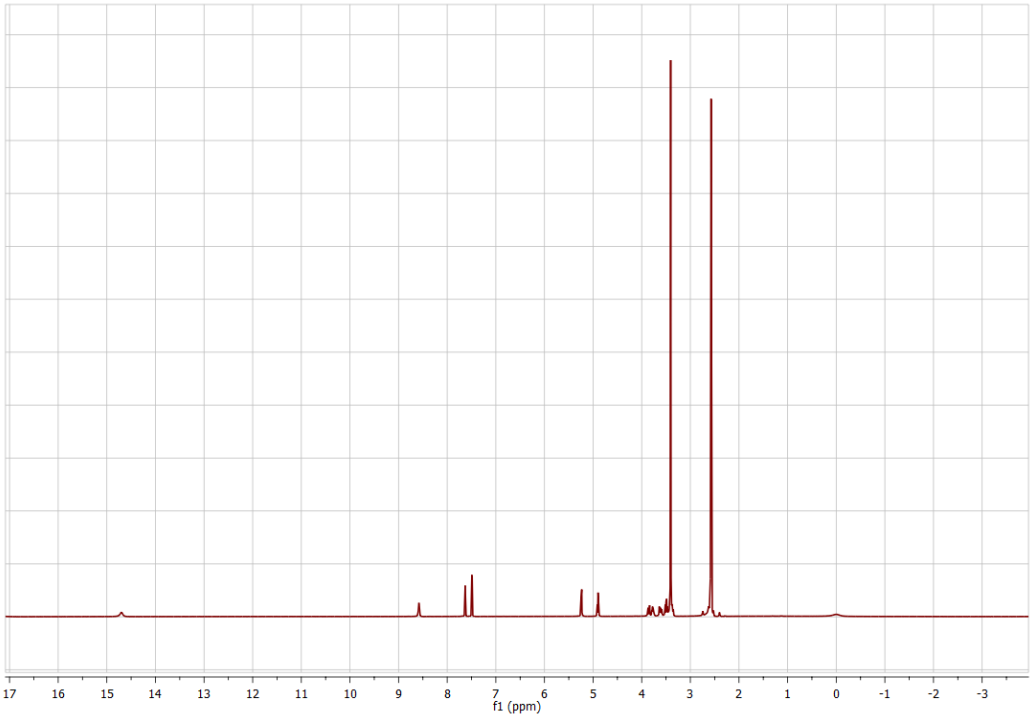

Fig. S10. ^{1}H NMR spectrum of **H*S*1** in DMSO-d_6.

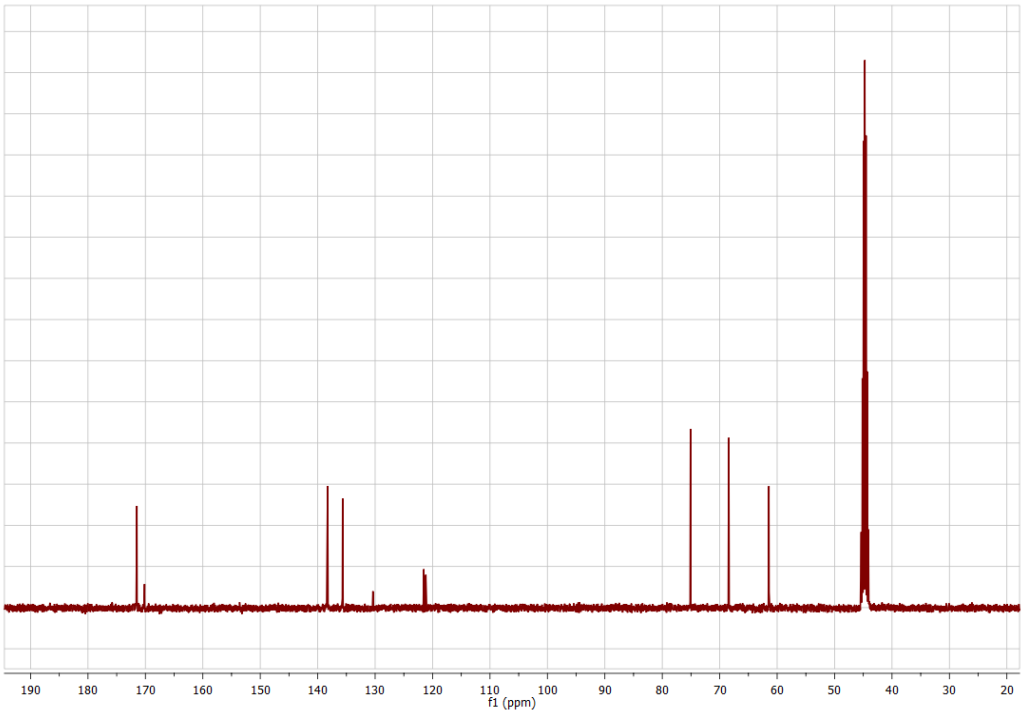

Fig. S11. ^{13}C NMR spectrum of **H*S*2** in DMSO-d_6.

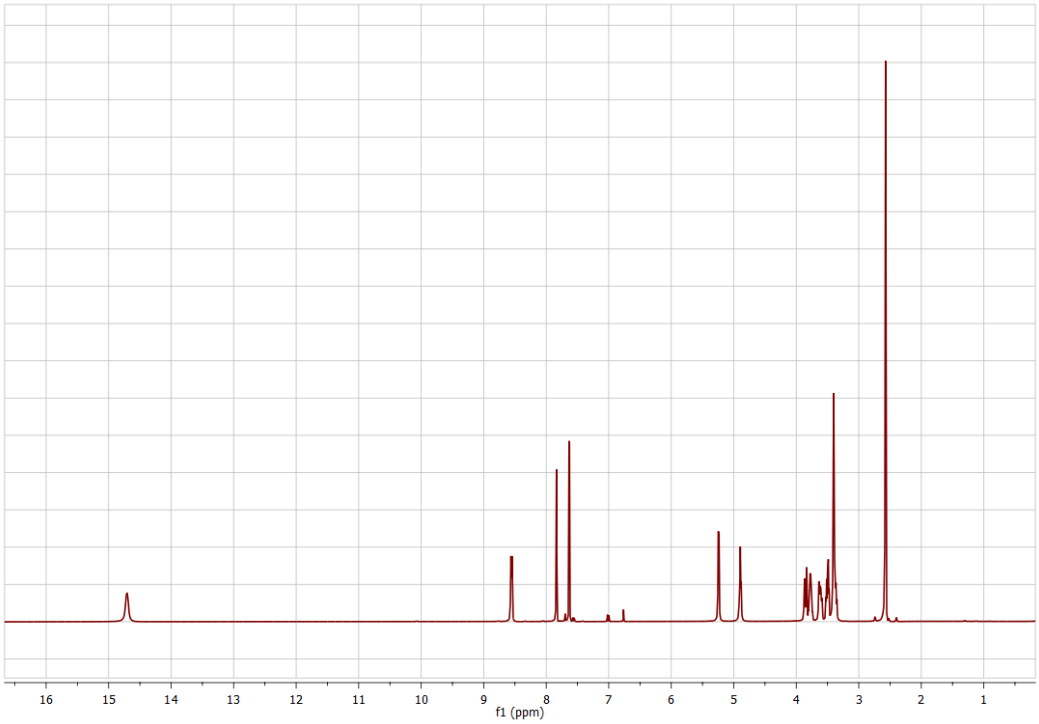

Fig. S12. ^{1}H NMR spectrum of **H*S*2** in DMSO-d_6.

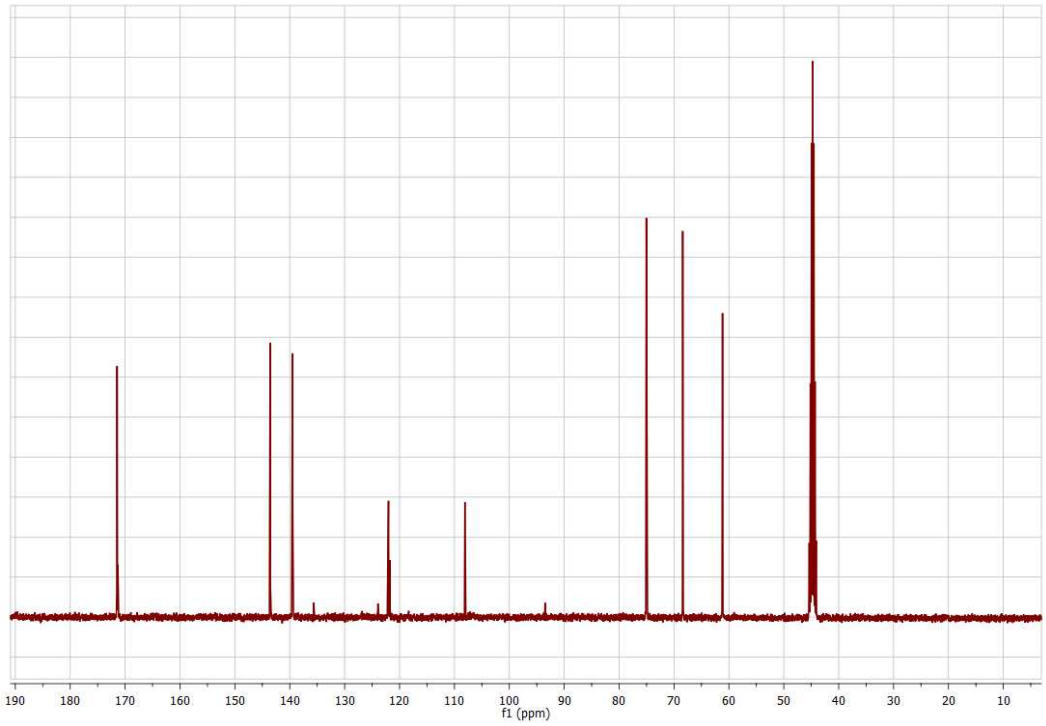

Fig. S13. ^{13}C NMR spectrum of **H*S*2** in DMSO-d_6.

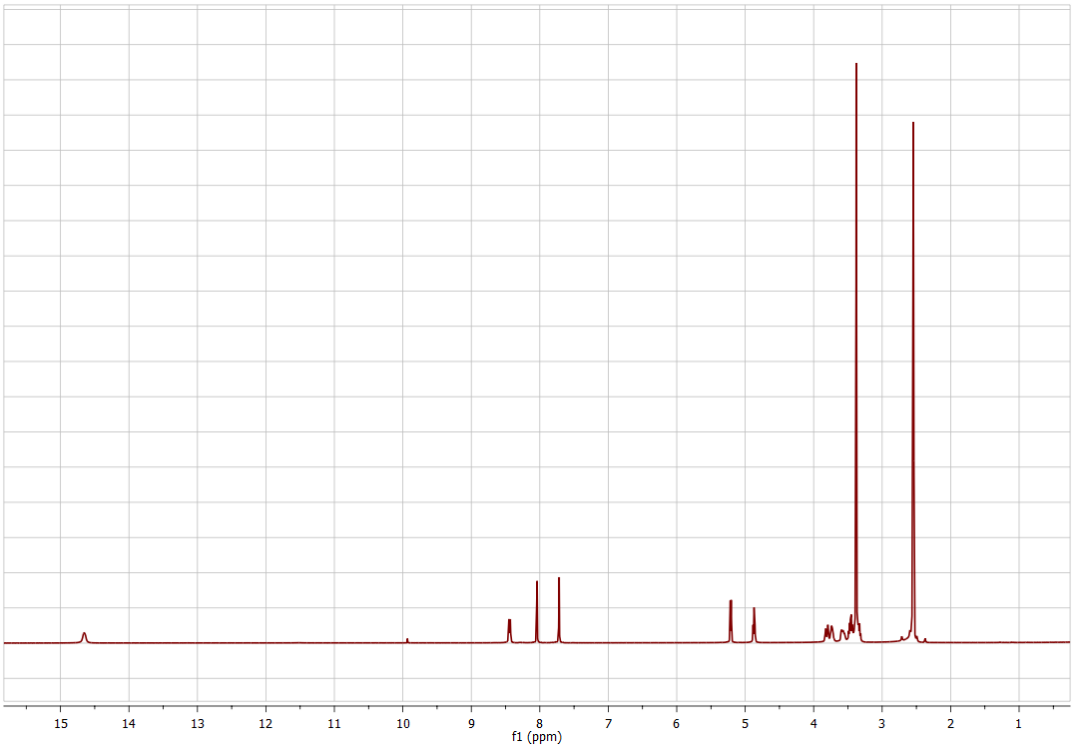

Fig. S14. ^{1}H NMR spectrum of **H*S*3** in DMSO-d_6.

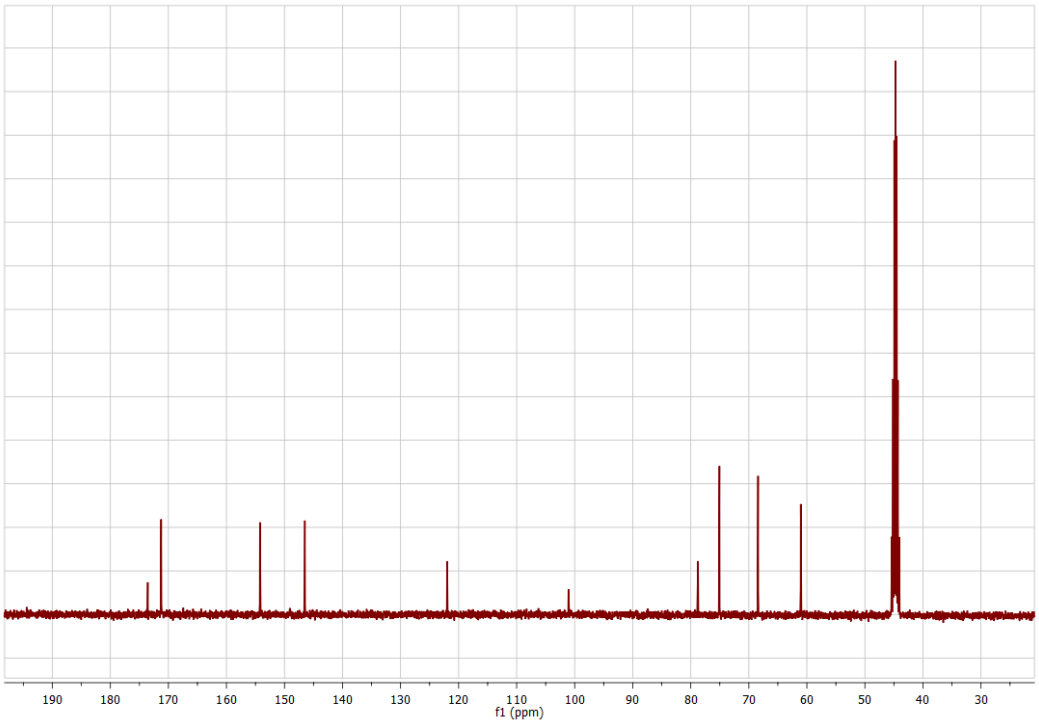

Fig. S15. ^{13}C NMR spectrum of **H*S*3** in DMSO-d_6.

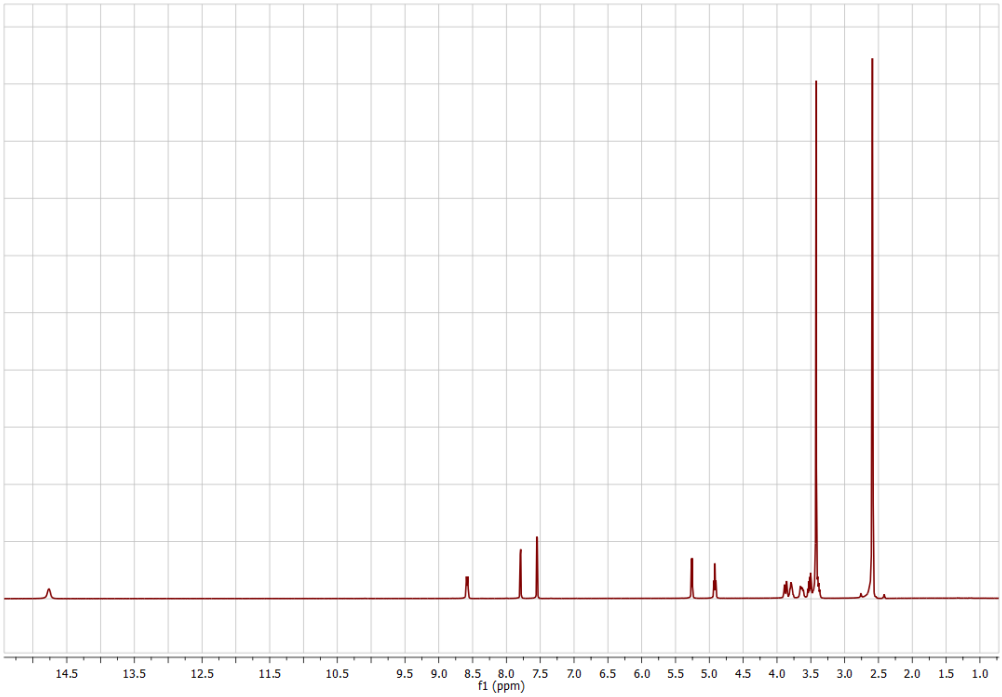

Fig. S16. ^{1}H NMR spectrum of **H*S*4** in DMSO-d_6.

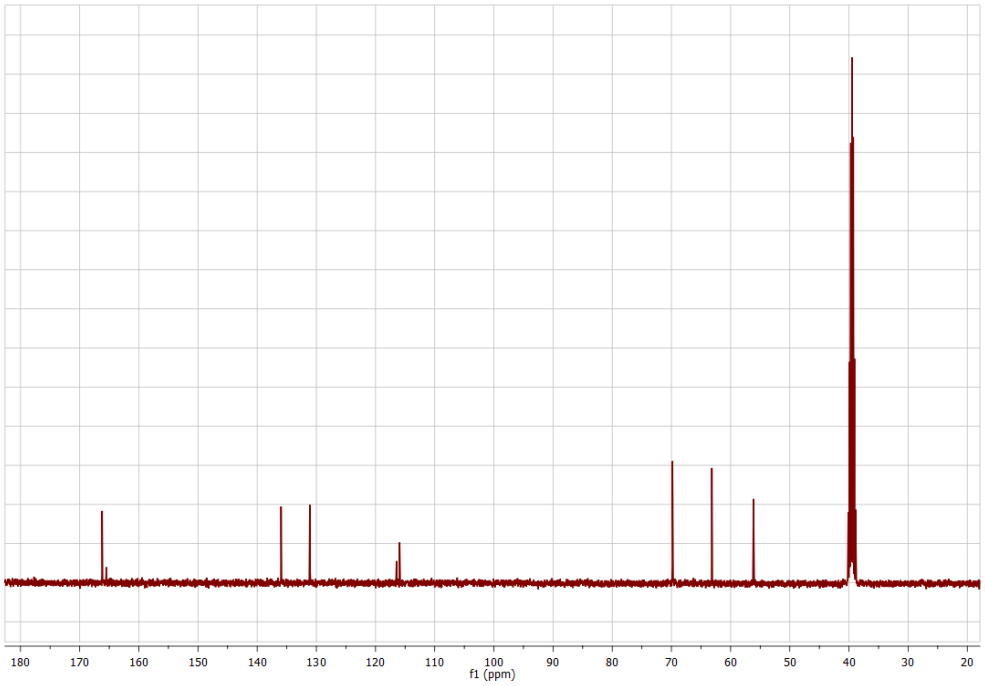

Fig. S17. ^{13}C NMR spectrum of **H*S*4** in DMSO-d_6.

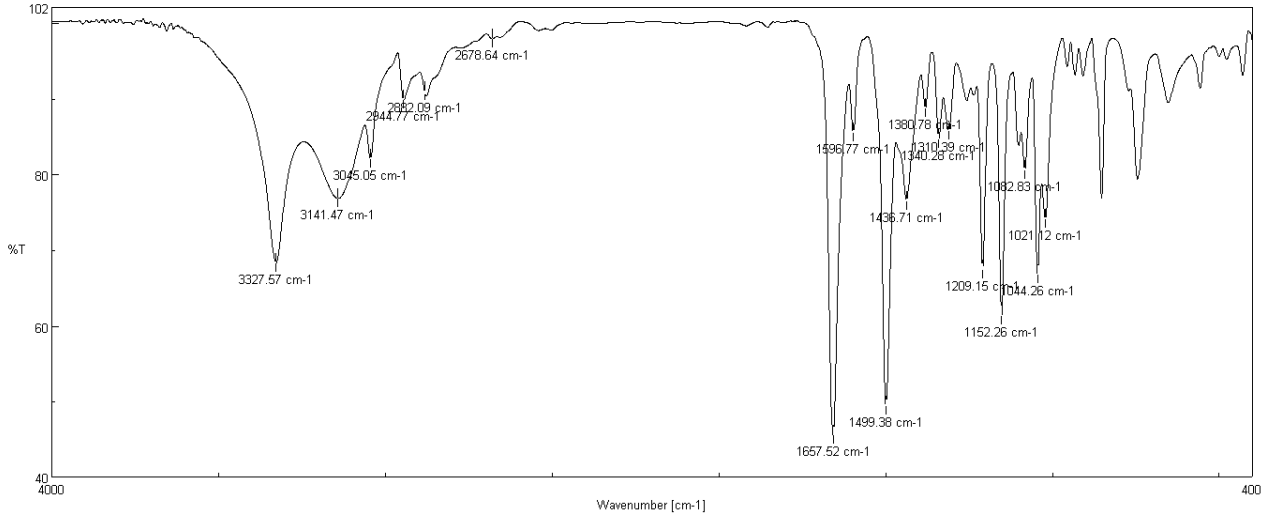

Fig. **S18** IR spectrum of **H*R*1**.

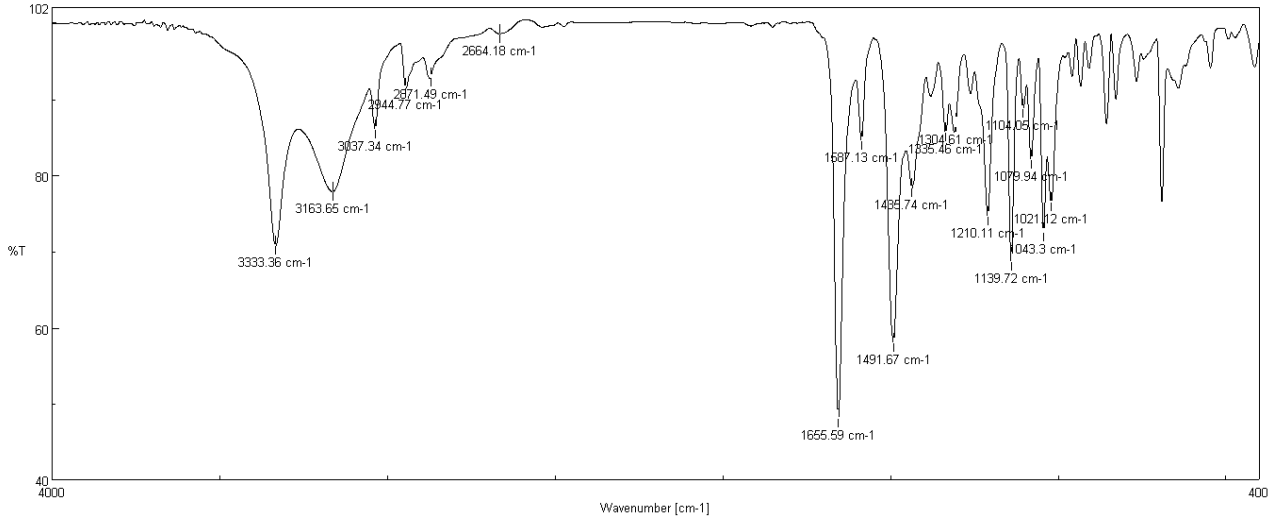

Fig. **S19** IR spectrum of **H*R*2**.

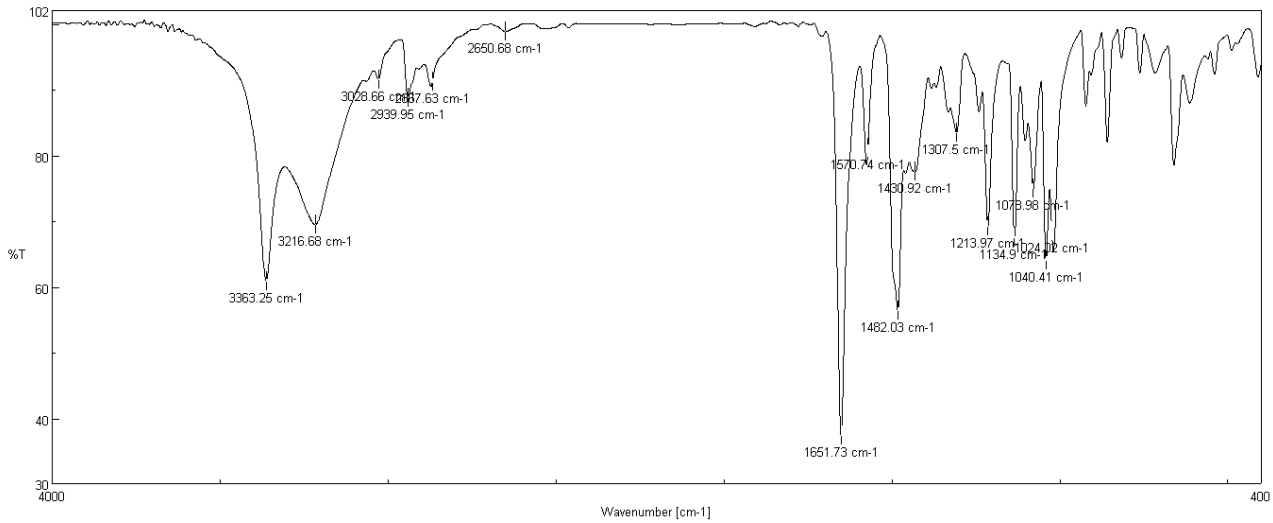

Fig. **S20** IR spectrum of **H*R*3**.

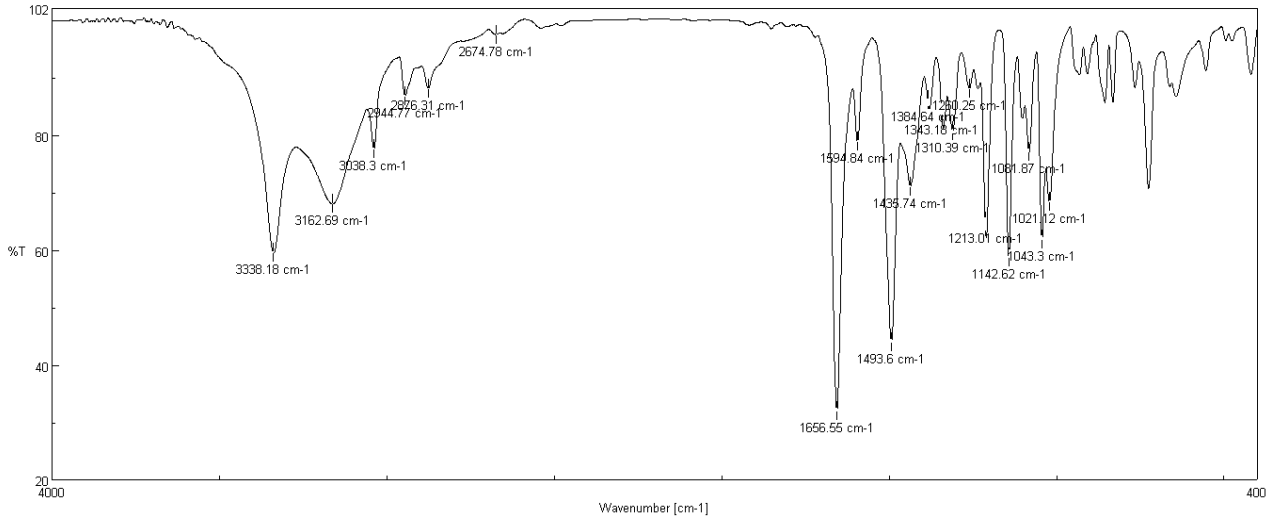

Fig. **S21** IR spectrum of **H*R*4**.

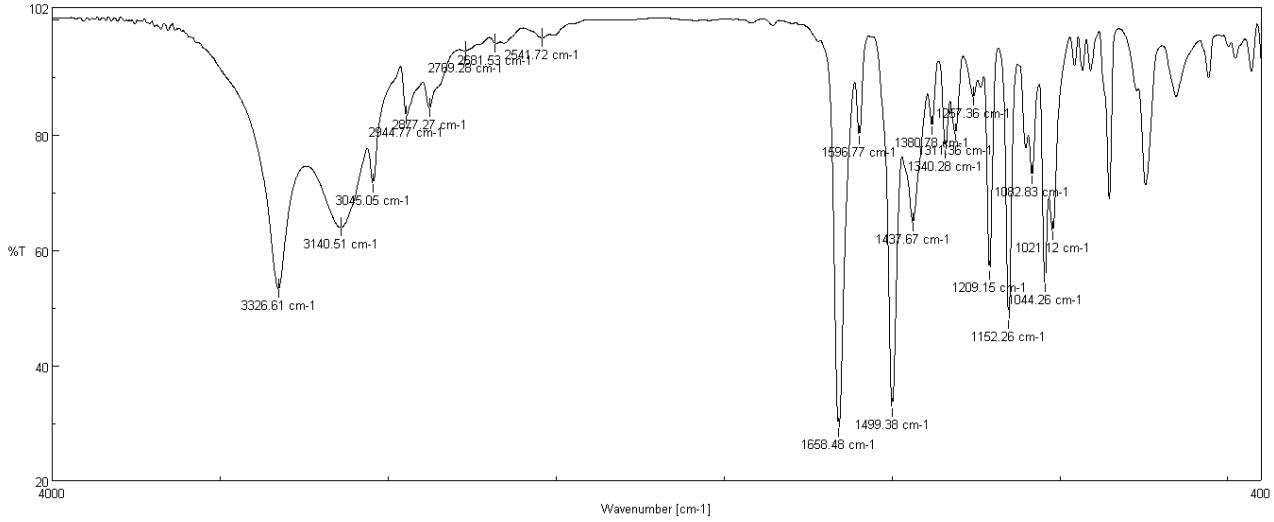

Fig. **S22** IR spectrum of **H*S*1**.

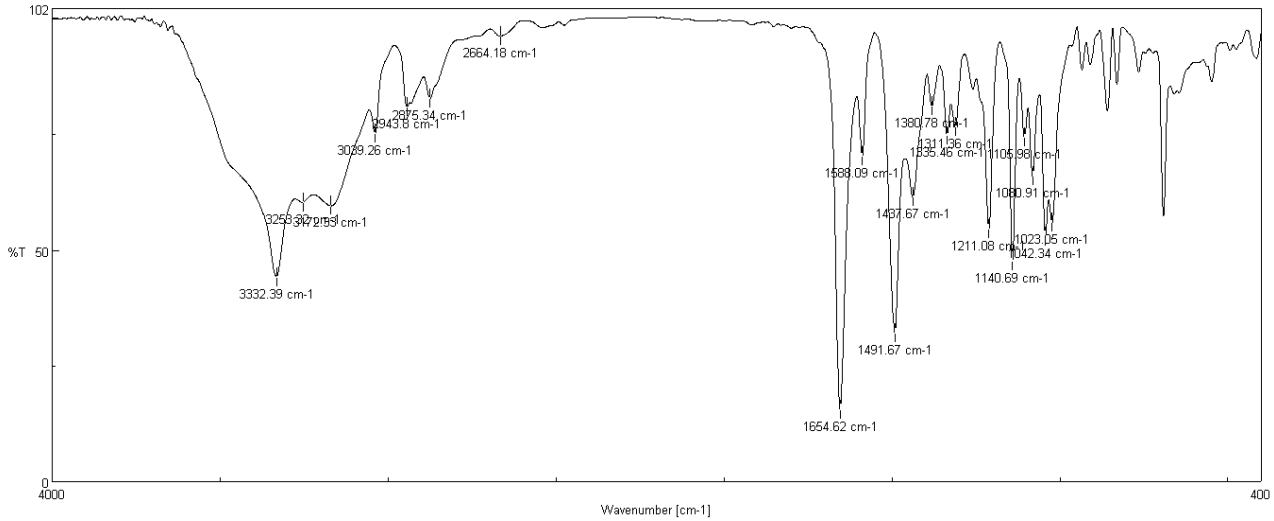

Fig. **S23** IR spectrum of **H*S*2**.

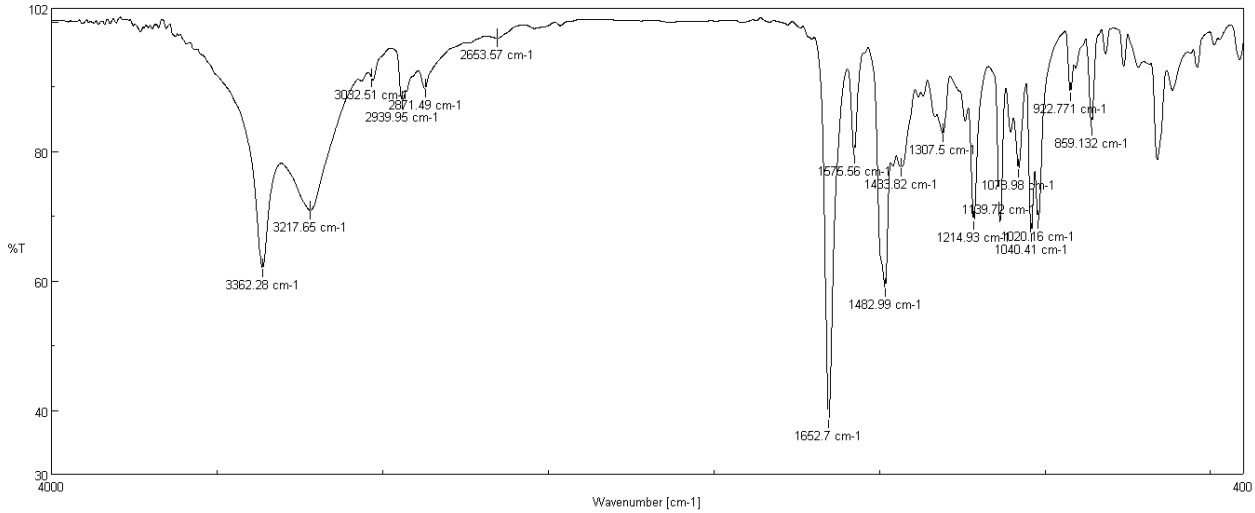

Fig. **S24** IR spectrum of **H*S*3**.

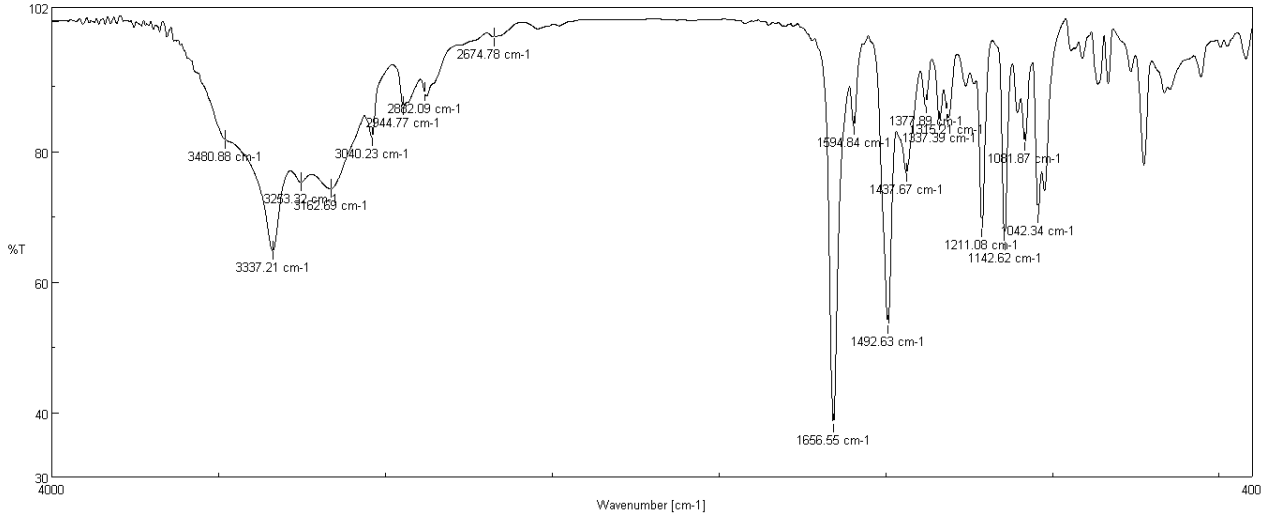

Fig. **S25** IR spectrum of **H*S*4**.

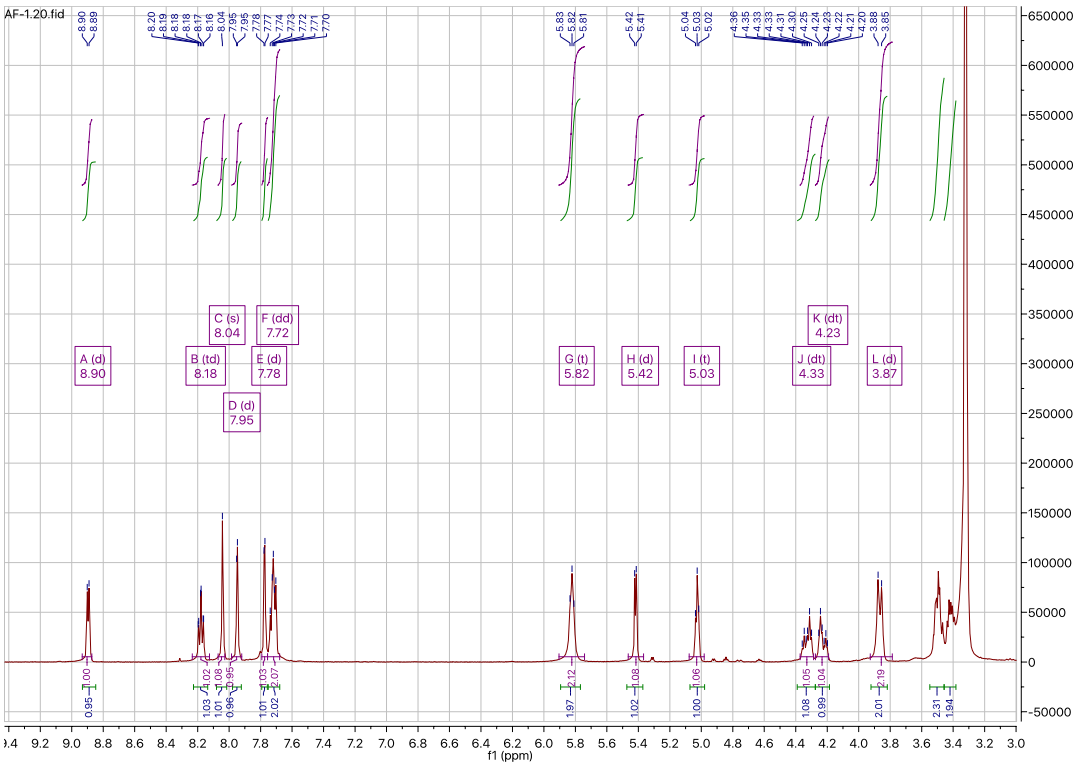

Fig. S26 ^{1}H NMR spectrum of **J1** in DMSO-d_6.

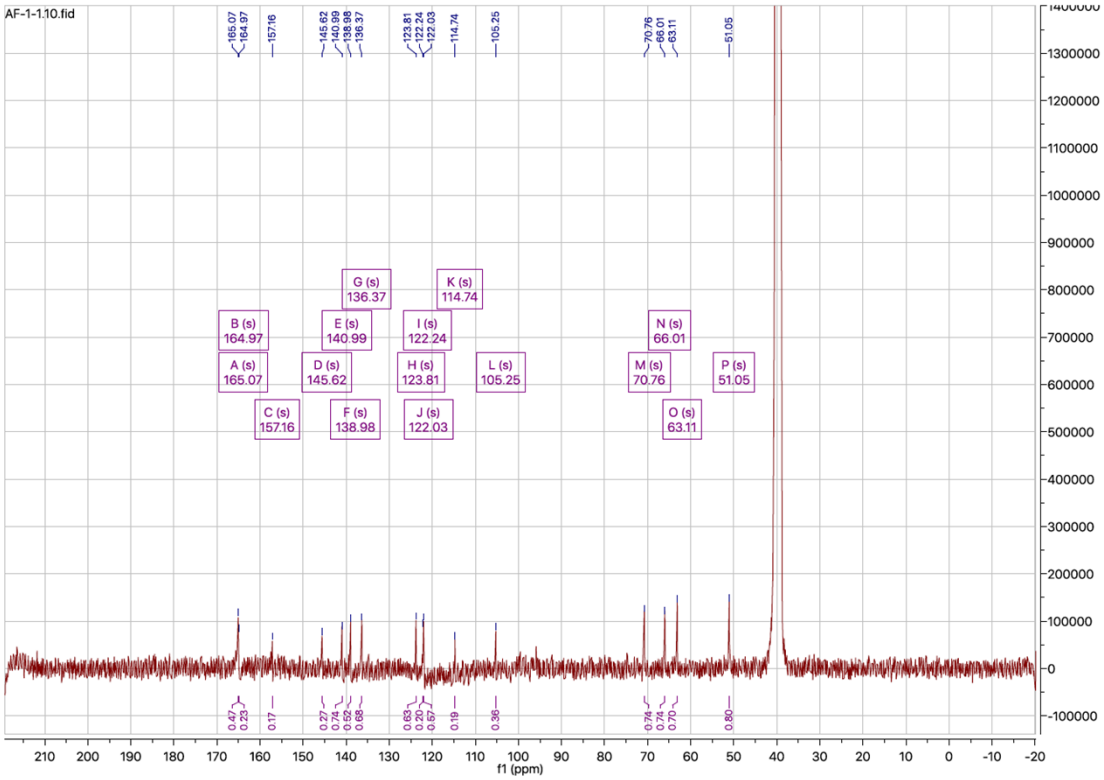

Fig. S27 ^{13}C NMR spectrum of **J1** in DMSO-d_6.

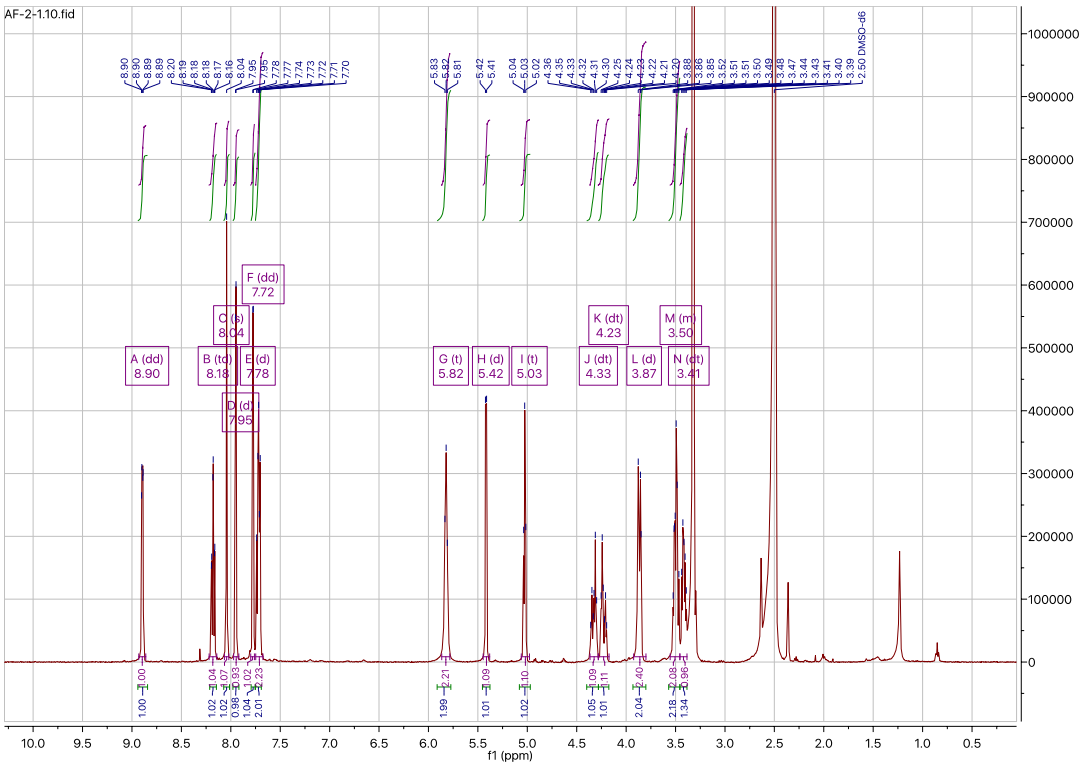

Fig. S28 ^{1}H NMR spectrum of **J2** in DMSO-d_6.

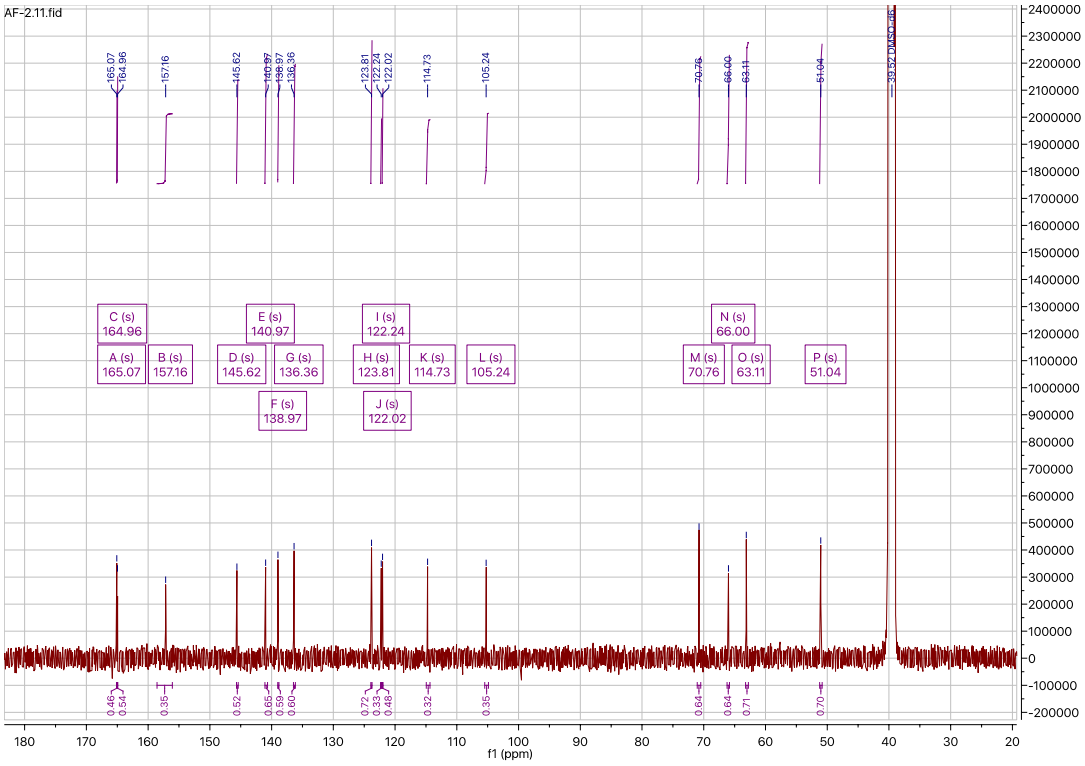

Fig. S29 ^{13}C NMR spectrum of **J2** in DMSO-d_6.

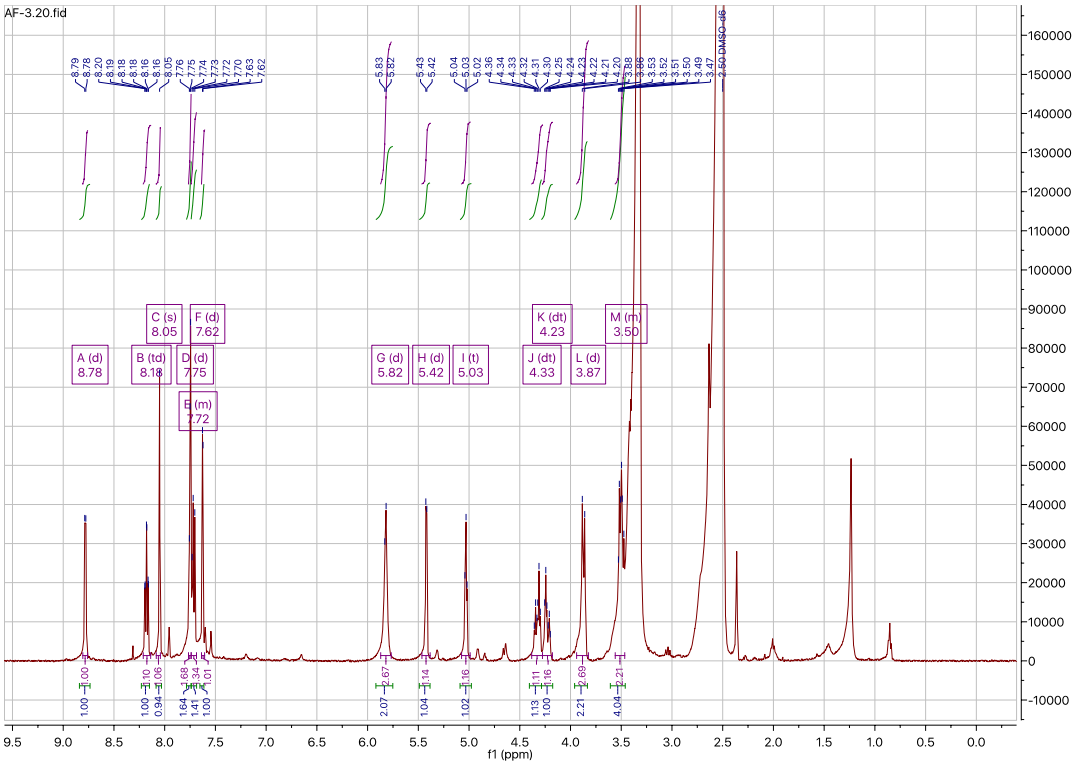

Fig. S30 ^{1}H NMR spectrum of **J3** in DMSO-d_6.

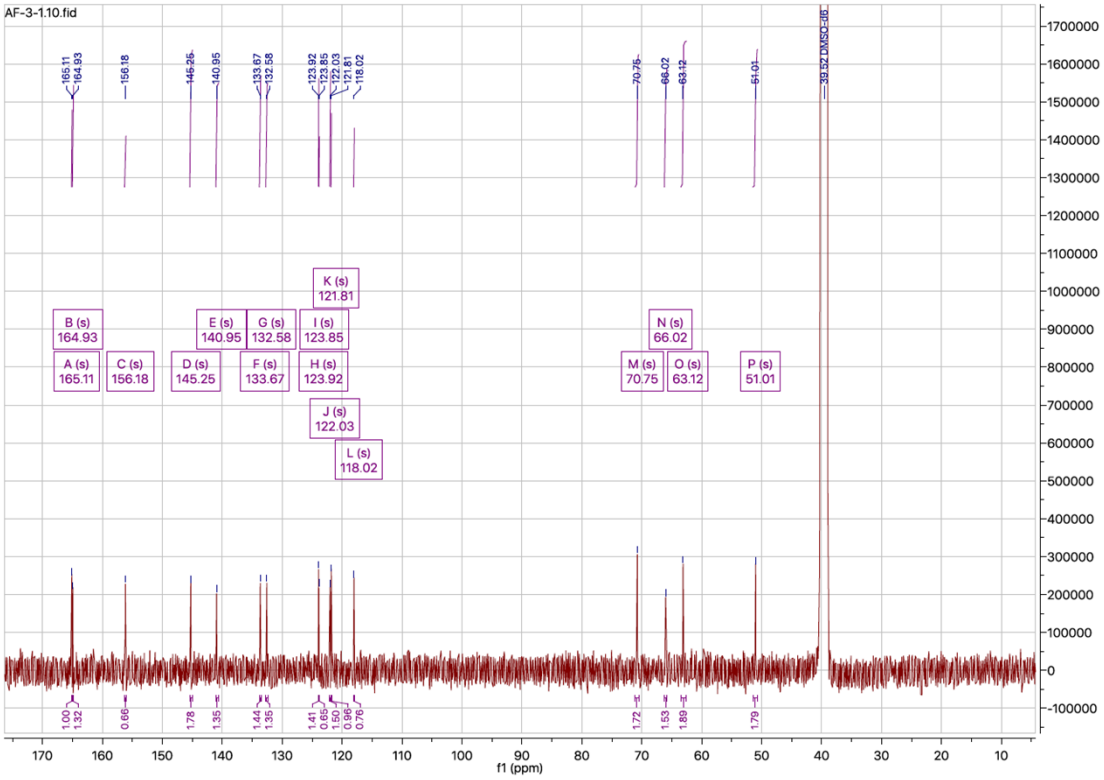

Fig. S31 ^{13}C NMR spectrum of **J3** in DMSO-d_6.

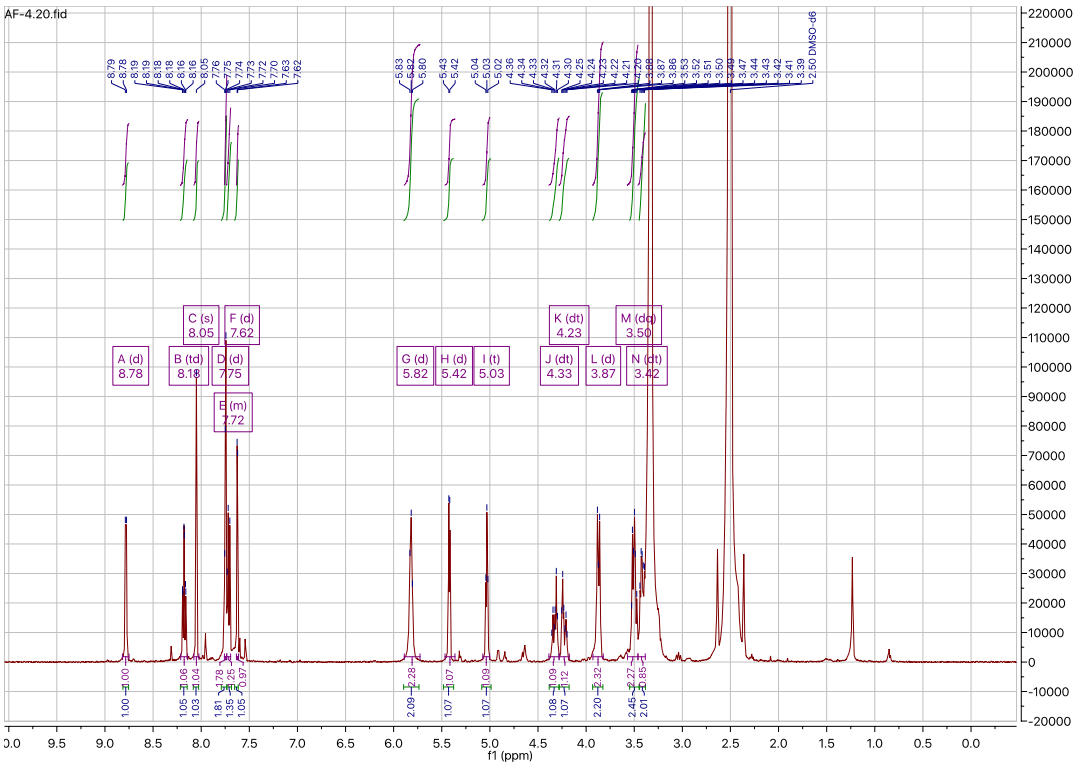

Fig. S32 ^{1}H NMR spectrum of **J4** in DMSO-d_6.

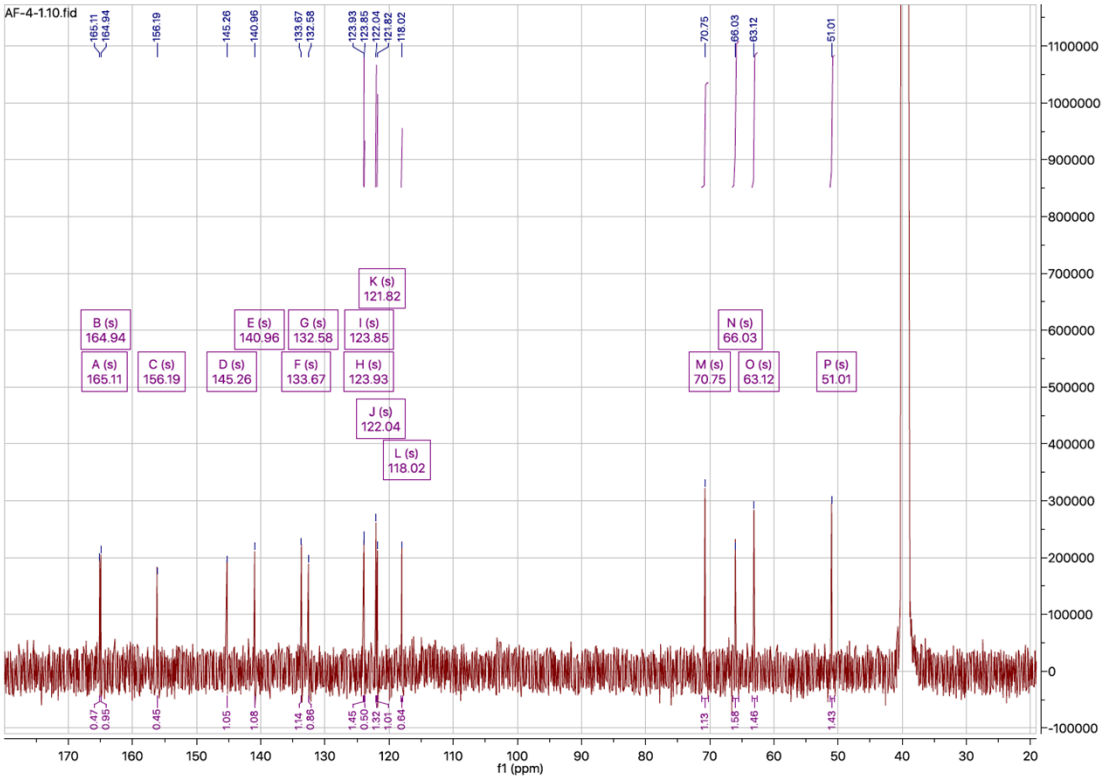

Fig. S33 ^{13}C NMR spectrum of **J4** in DMSO-d_6.

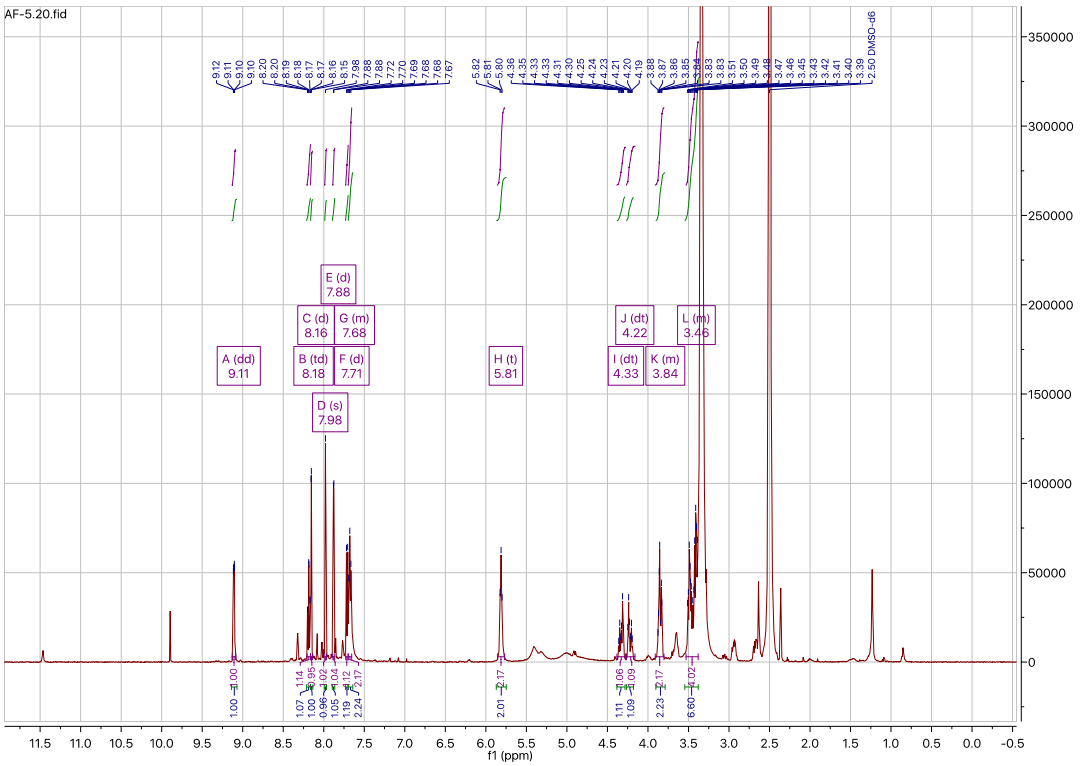

Fig. S34 ^{1}H NMR spectrum of **J5** in DMSO-d_6.

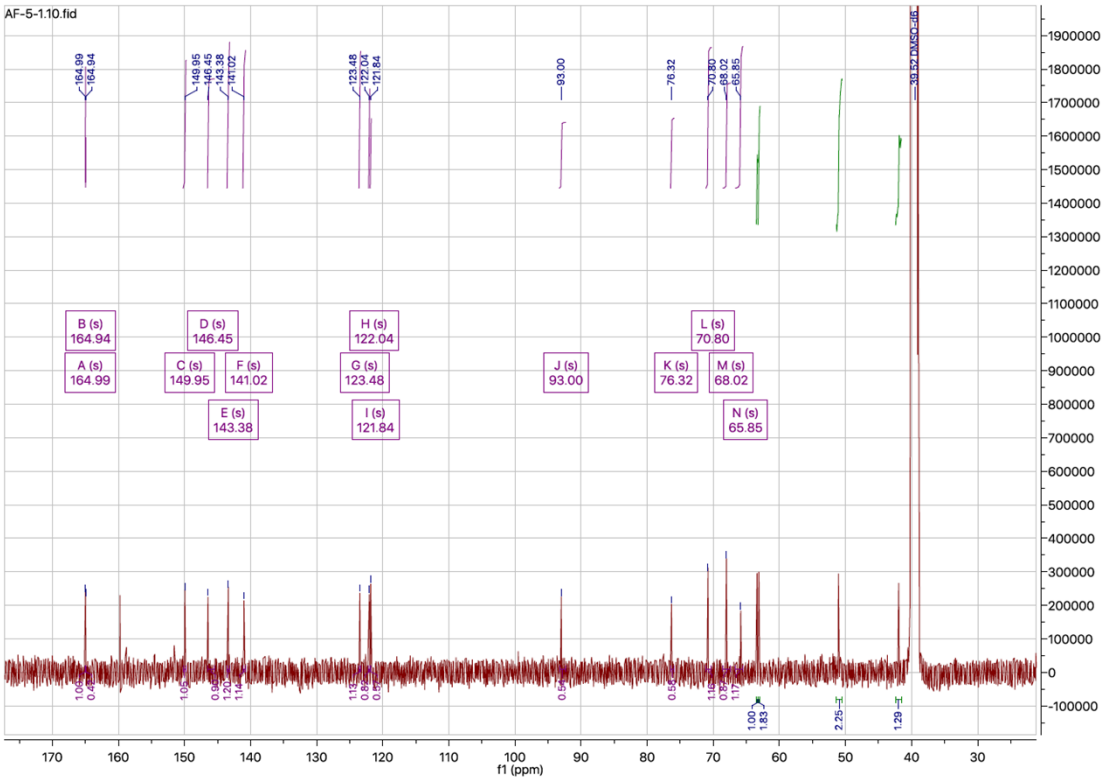

Fig. S35 ^{13}C NMR spectrum of **J5** in DMSO-d_6.

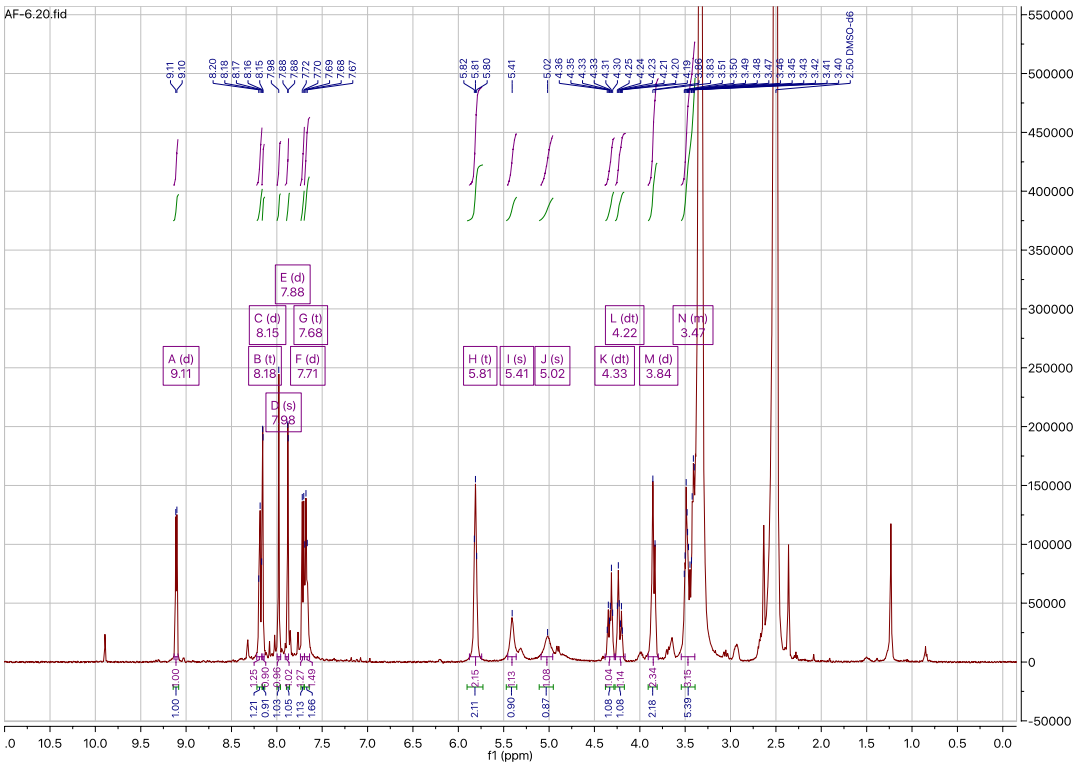

Fig. S36 ^{1}H NMR spectrum of **J6** in DMSO-d_6.

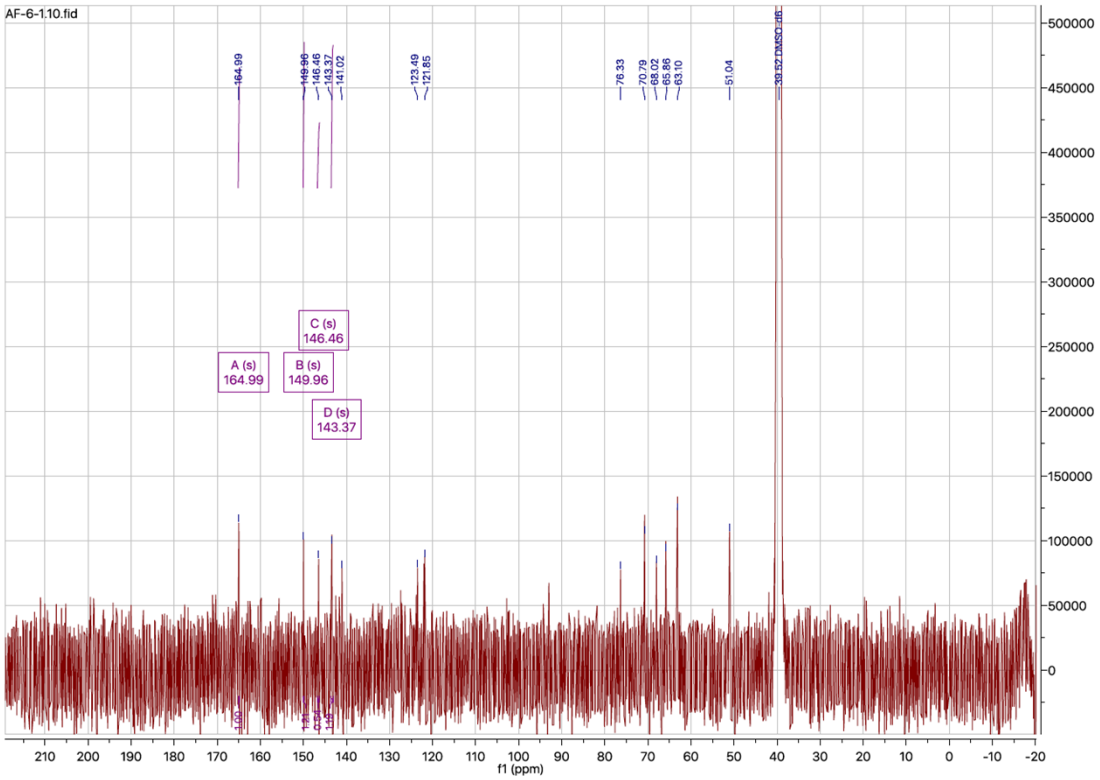

Fig. S37 ^{13}C NMR spectrum of **J6** in DMSO-d_6.

Fig. S38 ^{1}H NMR spectrum of **J7** in DMSO-d_6.

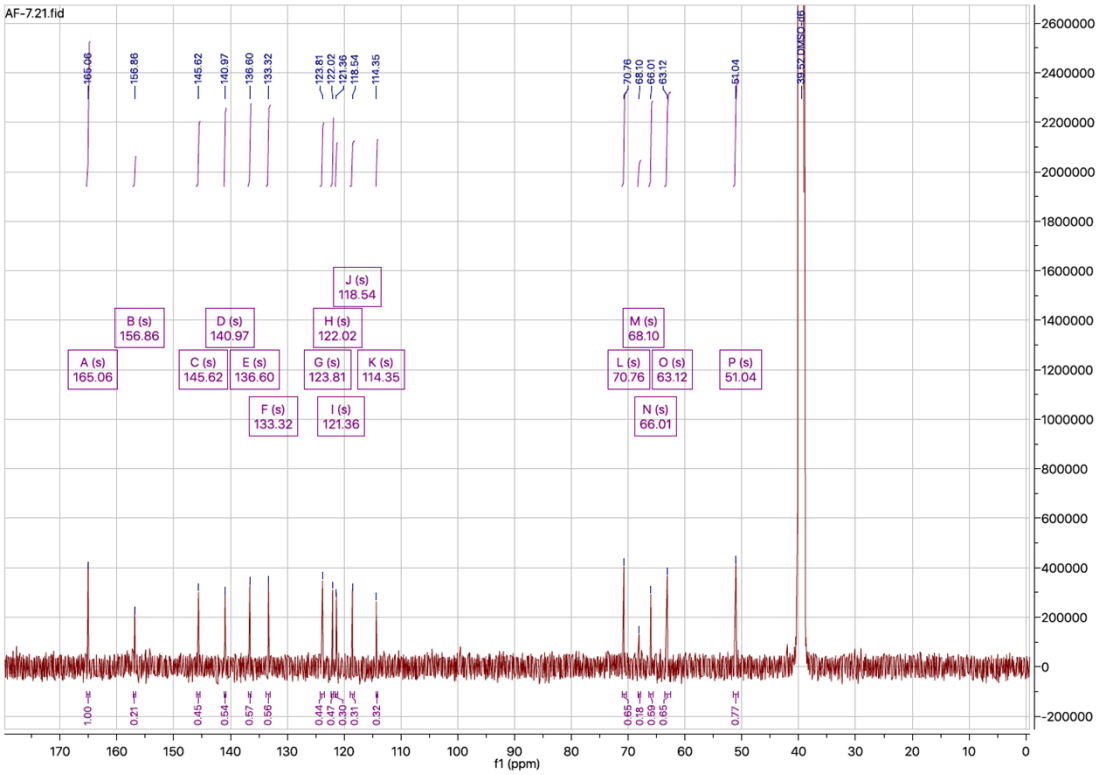

Fig. S39 ^{13}C NMR spectrum of **J7** in DMSO-d_6.

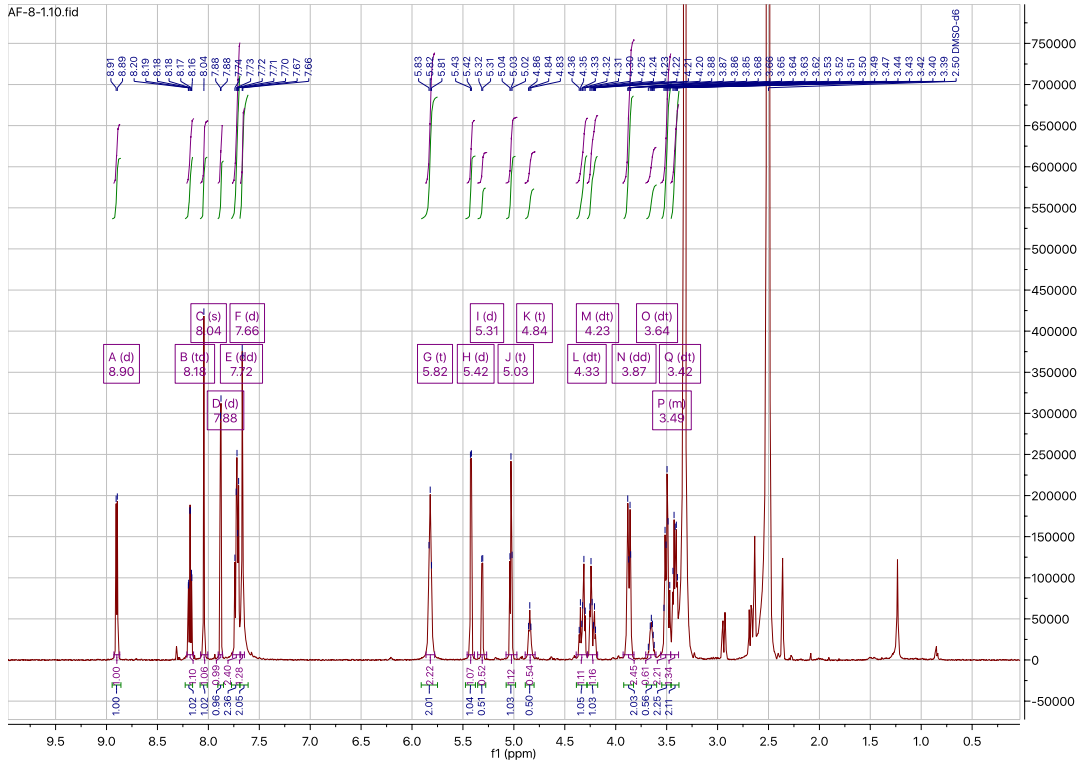

Fig. S40 ^{1}H NMR spectrum of **J8** in DMSO-d_6.

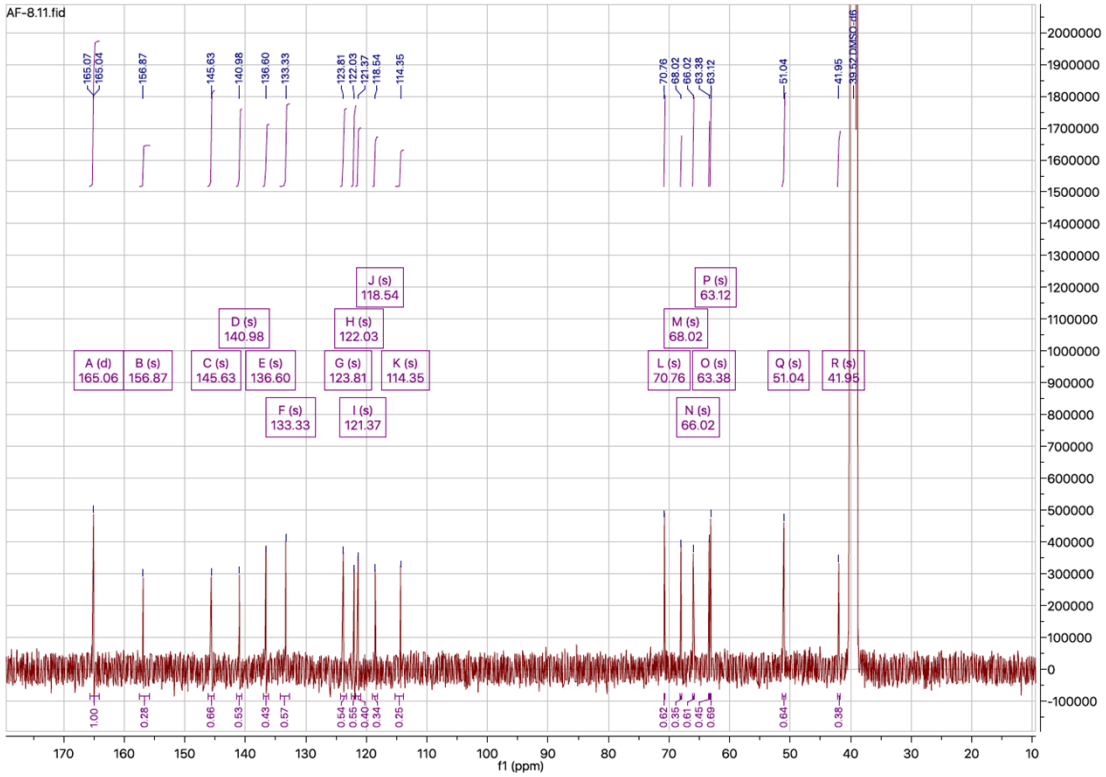

Fig. S41 ^{13}C NMR spectrum of **J8** in DMSO-d_6.

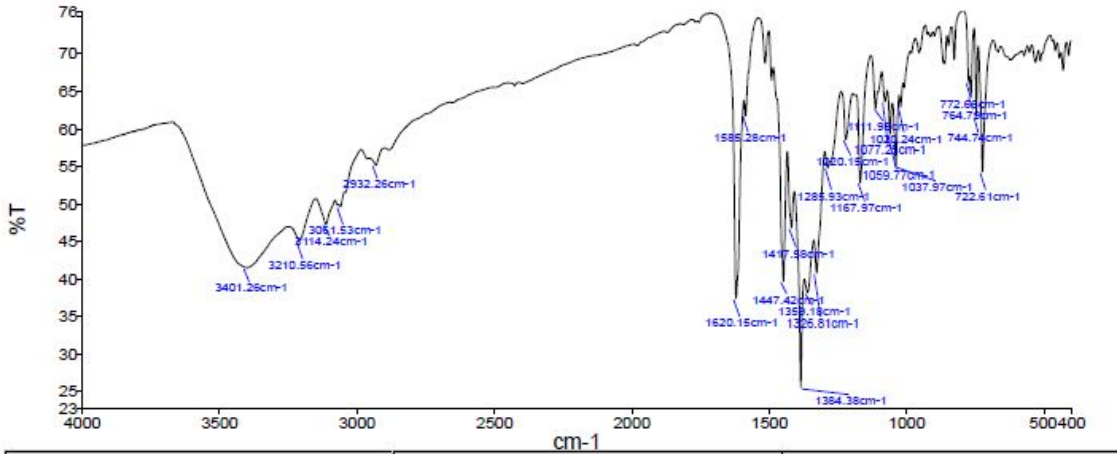

Fig. **S42** IR spectrum of **J1**

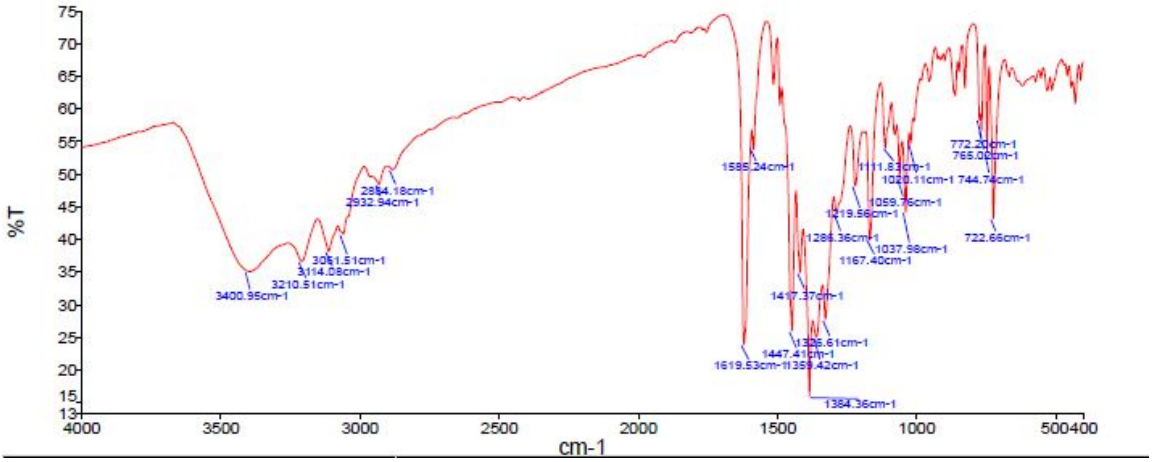

Fig. **S43** IR spectrum of **J2**

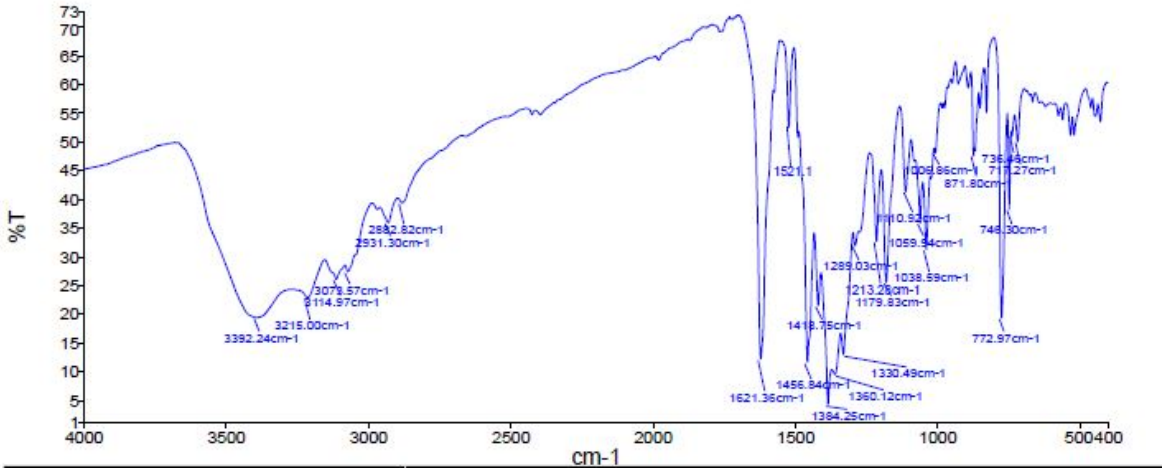

Fig. **S44** IR spectrum of **J3**

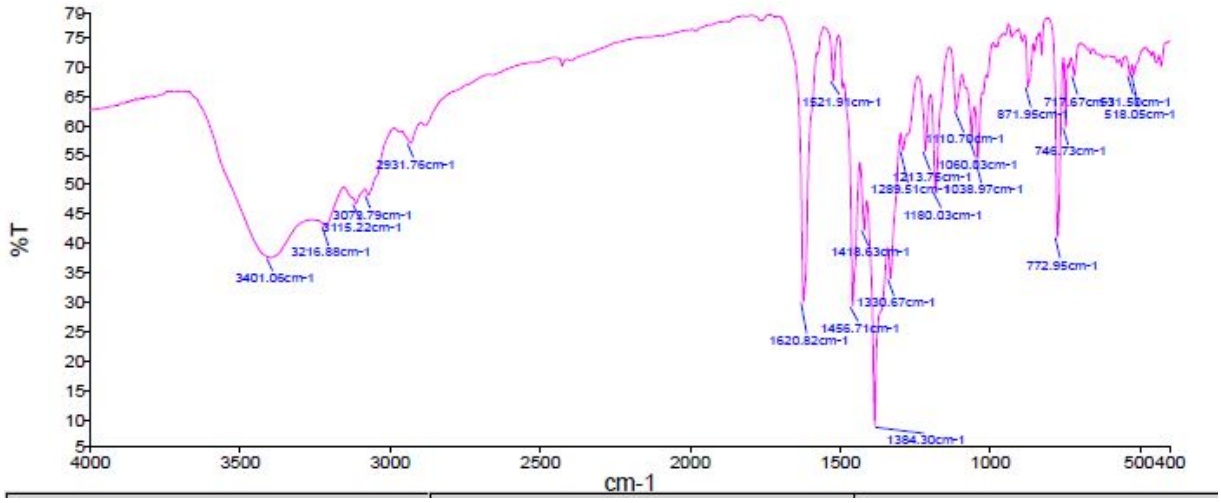

Fig. **S45** IR spectrum of **J4**

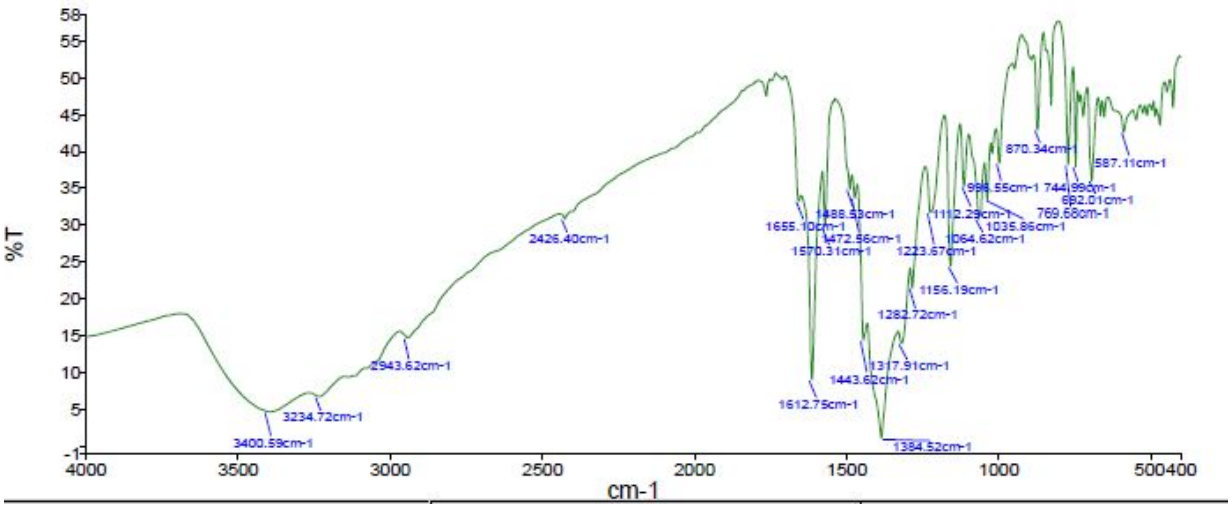

Fig. **S46** IR spectrum of **J5**

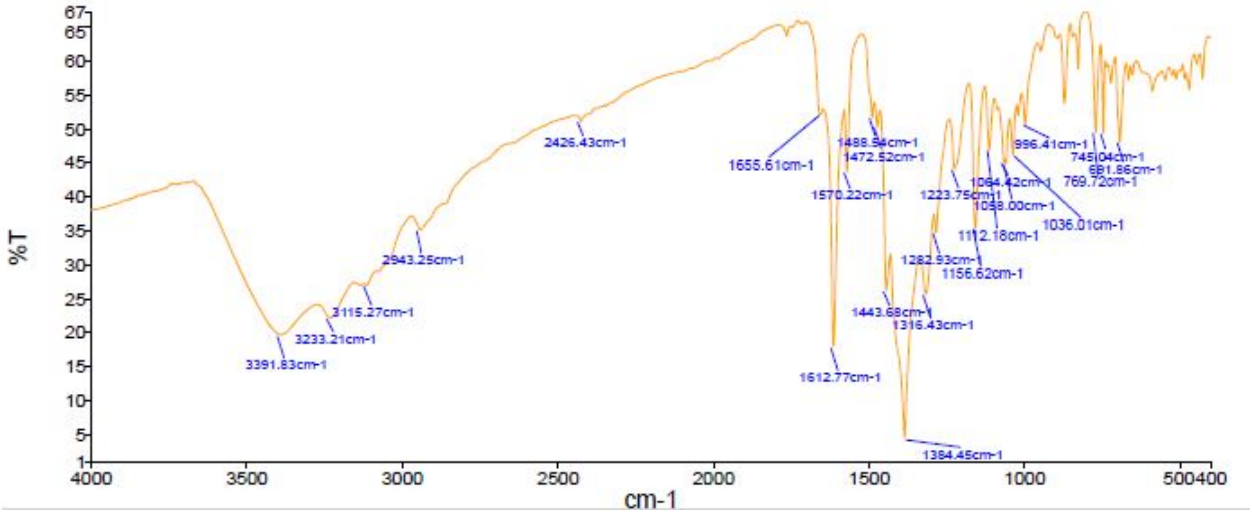

Fig. **S47** IR spectrum of **J6**

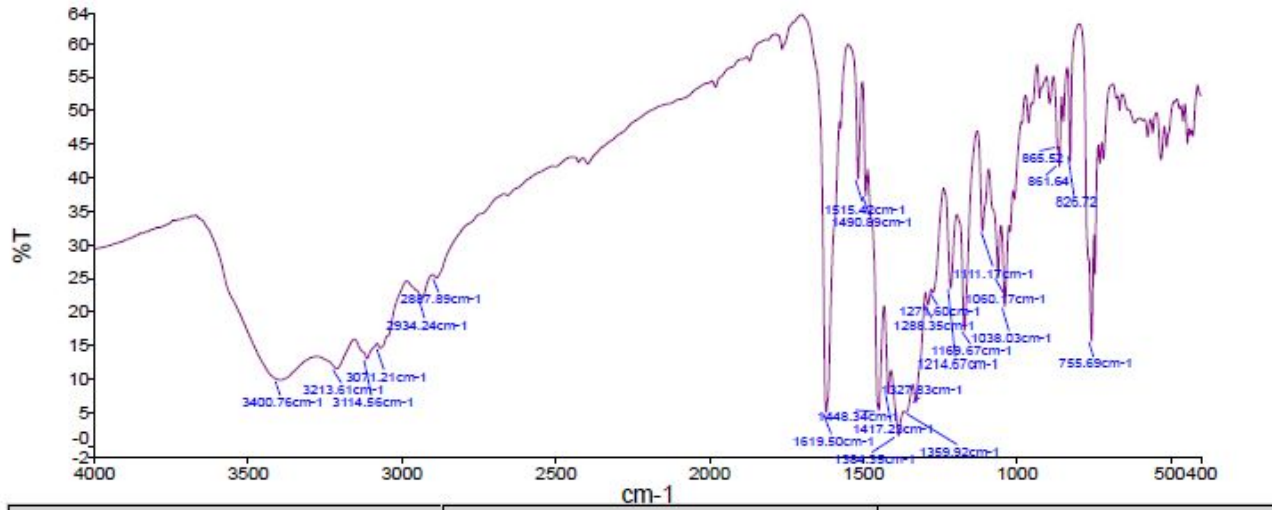

Fig. **S48** IR spectrum of **J7**

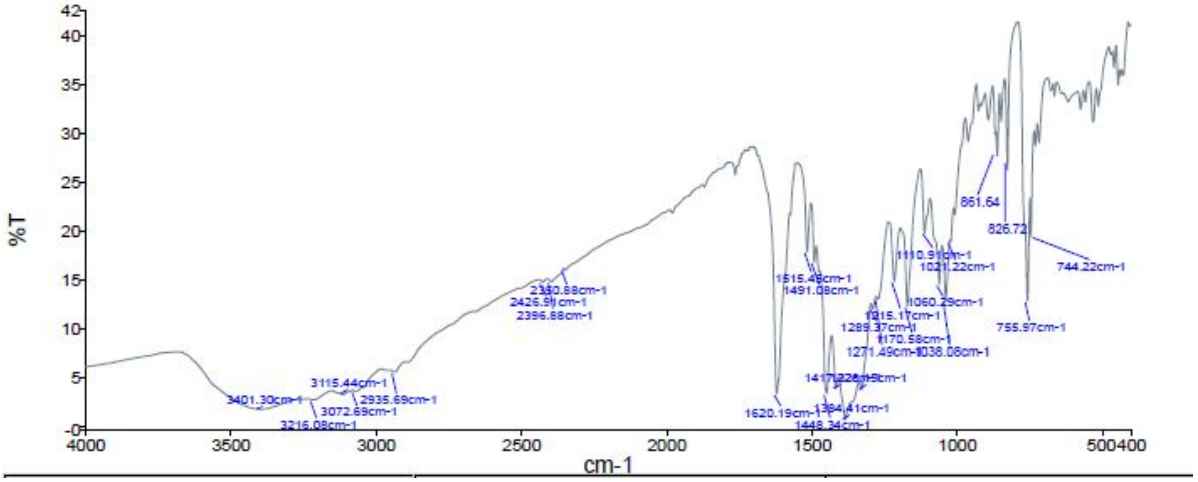

Fig. **S49** IR spectrum of **J8**

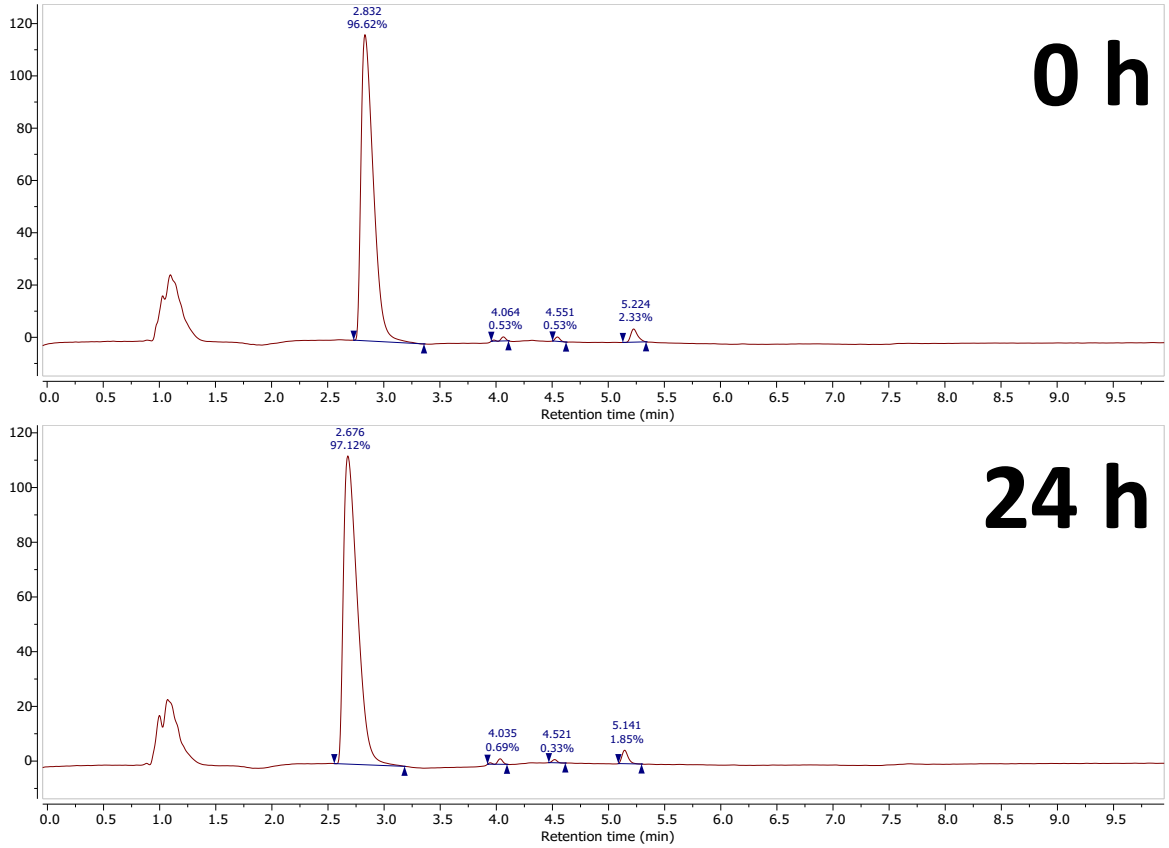

Fig. S50: LC/MS spectrum of **J4** in PBS buffer (pH = 7.4).

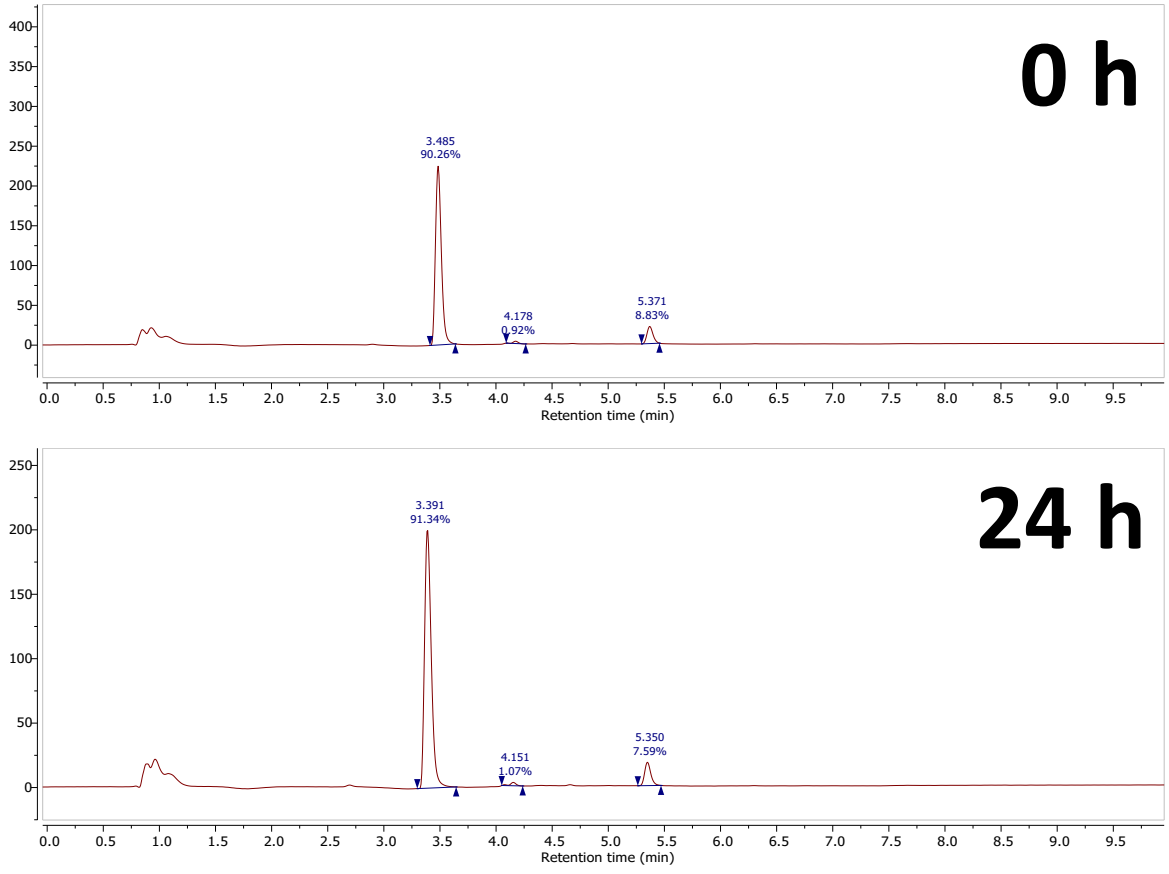

Fig. S51: LC/MS spectrum of **J4** in proteasome assay buffer (pH = 7.4).

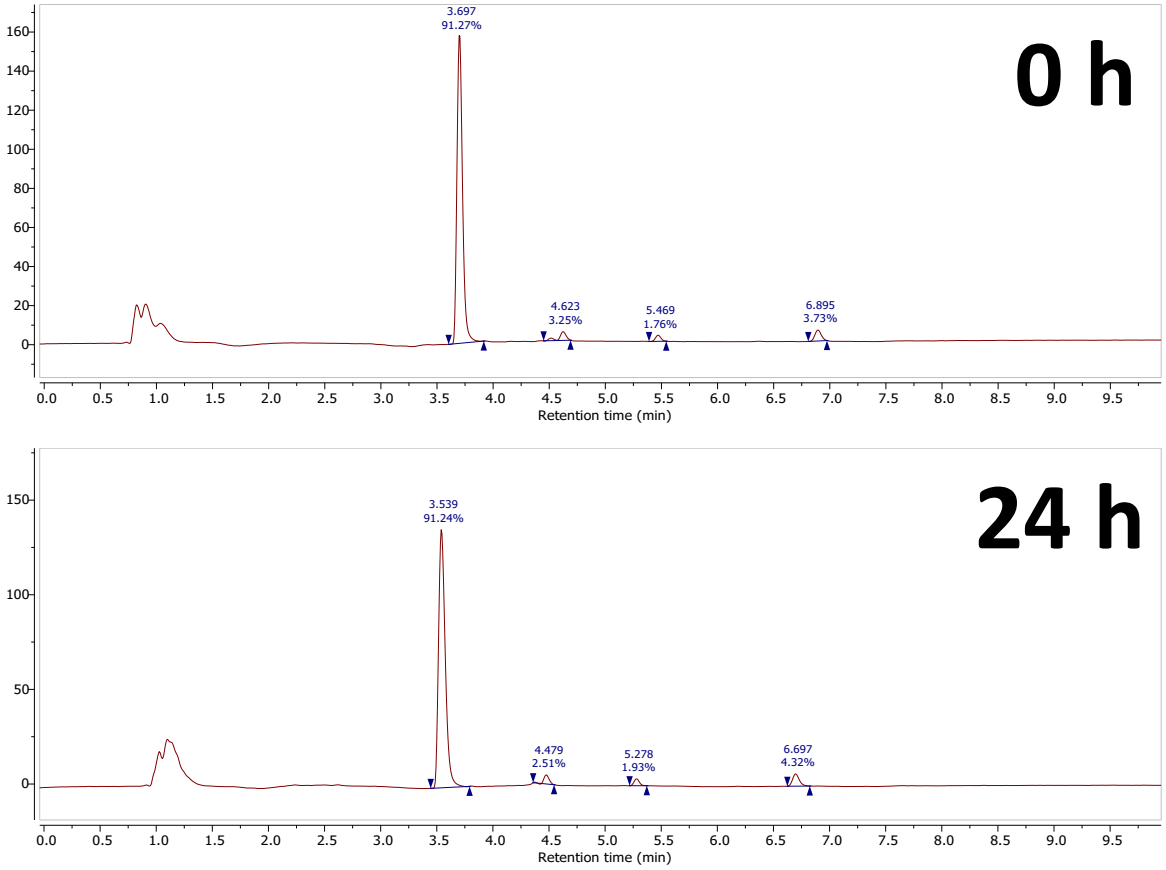

Fig. S52: LC/MS spectrum of **J6** in PBS buffer (pH = 7.4).

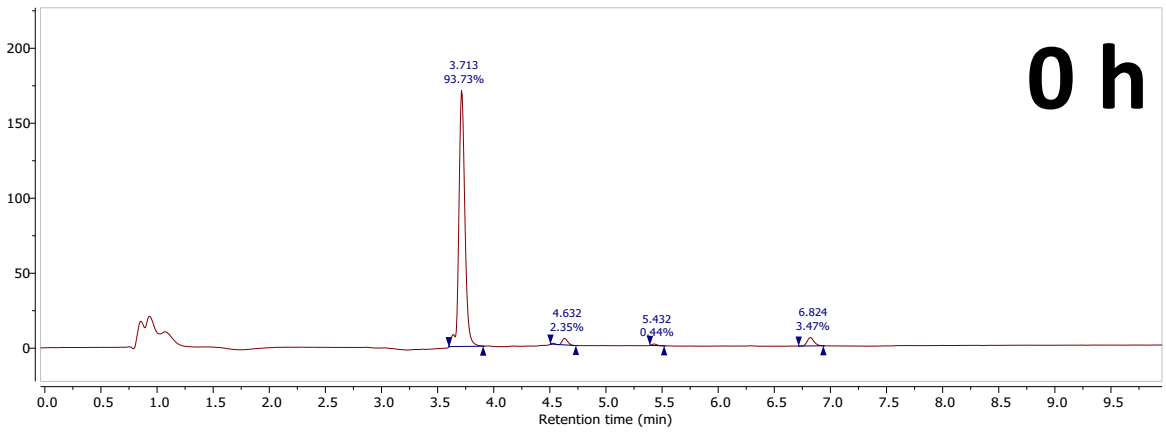

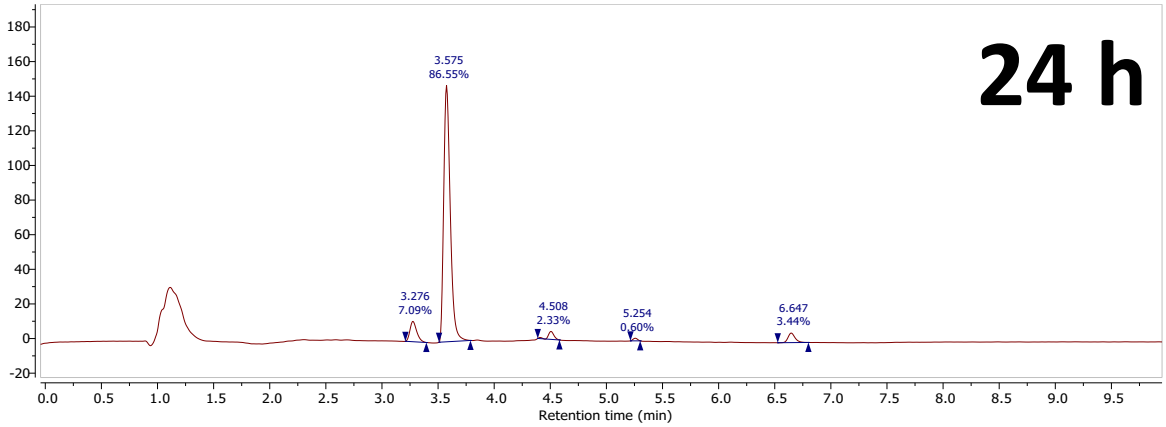

Fig. **S53: LC/MS** spectrum of **J6** in proteasome assay buffer (pH = 7.4).

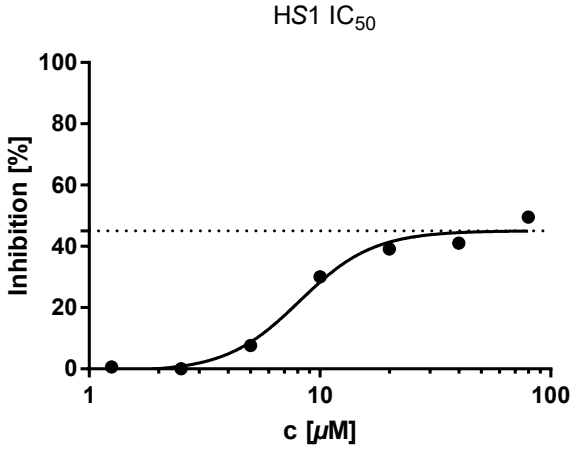

Fig. **S54:** Concentration-response curve of **HS1** (*i.e*. J4 ligand) towards 20S proteasome inhibition.

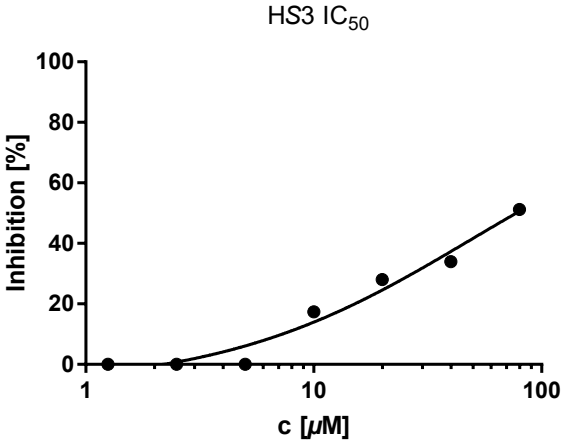

Fig. **S55:** Concentration-response curve of **HS3** (*i.e*. J6 ligand) towards 20S proteasome inhibition.

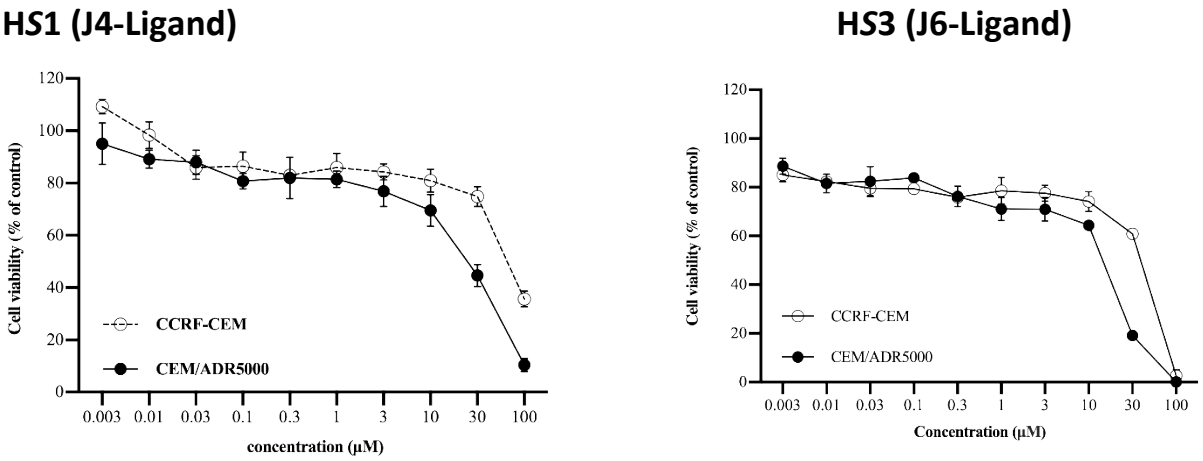

Fig. S56. Concentration-response curves of the Schiff base ligands **H*S*1** and **H*S*3** (for the Pd(II) complexes **J4** and **J6**, respectively) towards CCRF-CEM and CEM/ADR5000 cells. Resazurin assays were performed three times at 37 °C for 72 h.

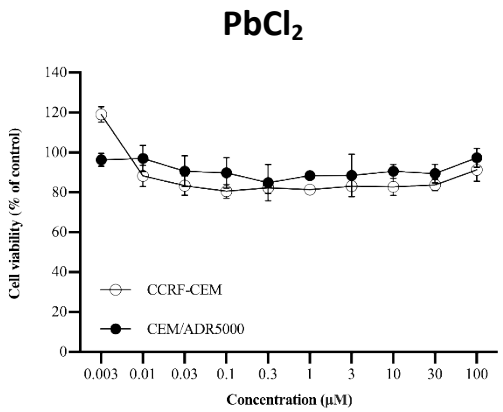

Fig. S56. Concentration-response curves of the palladium salt **$PbCl_2$** towards CCRF-CEM and CEM/ADR5000 cells. Resazurin assays were performed three times at 37 °C for 72 h.